

# Achieving Downstream Fairness with Geometric Repair

KWEKU KWEGYIR-AGGREY\*, JESSICA DAI\*, JOHN P. DICKERSON, and KEEGAN HINES, Arthur AI, USA

Consider a scenario where some “upstream” model developer must train a fair model, but is unaware of the fairness requirements of a “downstream” model user/stakeholder. In the context of fair classification, we present a technique that specifically addresses this setting, by post-processing a regressor’s scores such they yield fair classifications for any downstream choice in decision threshold. To begin, we leverage ideas from optimal transport to show how this can be achieved for binary protected groups across a broad class of fairness metrics. Then, we extend our approach to address the setting where a protected attribute takes on multiple values, by re-casting our technique as a convex optimization problem that leverages lexicographic fairness.

Additional Key Words and Phrases: fairness in machine learning, optimal transport, fair classification

## 1 INTRODUCTION

A common critique of fair algorithmic interventions is that they do not center real-world usage [35, 49]. In this work, we study a problem that exists in the gap between the design of “fair” machine learning interventions and their deployment in “in the wild”—a gap that exists due to the fact that the users of (fair) machine learning models are not always the people who created the tool. To illustrate this gap, we begin with a sketch of how machine learning tools are often used in the context of some sociotechnical pipeline where fairness is a concern. First, a model developer trains a machine learning model to make predictions about individuals based on past data. Typically, these decisions are made by taking the continuous outputs (or *scores*) from a model, such as predicted probabilities, and then using a cutoff (or *threshold*), a final classification decision (e.g. yes/no) is made based on whether the individual’s score was above or below the threshold. Once trained, the model is evaluated for bias and correctness. If the model exhibits bias, then some appropriate fairness intervention may be applied, and the model is modified or retrained to mitigate the observed bias. At the last stage, when the model is deployed for usage, the prior steps are repeated as necessary if new biases emerge.

In many cases, a machine learning pipeline similar to the one described above involves two parties: an “upstream” model developer who is responsible for creating and/or engineering the model, and a “downstream” user, stakeholder, or practitioner, who uses the model for decision-making [9, 24]. The upstream developer and downstream user are often different parties; the steps detailed above might be done only by the upstream model developer, while the downstream end-user must rely solely on the model provided by the developer. Furthermore, either party may be constrained by resources, logistical barriers, or context-specific barriers, leading the downstream model user to employ a different threshold for making final classification decisions than the upstream model developer had anticipated and optimized for [19, 26].

Consider the following example. Suppose a model developer validates the performance and fairness of their model by computing the Area Under the Curve (AUC) for each protected group. AUC scores, which fall between 0 and 1, are computed by aggregating false positive and true positive rates across all possible thresholds used to make classification decisions. In many domains, a model is said to be “good,” i.e. usable, if its AUC is above 0.8 [1]. In this case, if all groups have an AUC above 0.8, the model is deemed to be “fair” and perform well. However, AUC measures performance across

\*Both authors contributed equally to this research.

Authors’ address: Kweku Kwegyir-Aggrey, kweku@arthur.ai; Jessica Dai, jessica@arthur.ai; John P. Dickerson, john@arthur.ai; Keegan Hines, keegan@arthur.ai, Arthur AI, USA.

all thresholds. This means that for a single choice in threshold, a model could perform poorly for only one group despite a relatively high overall or group-wise AUC. In the context of the pipeline described above, the model *user* ultimately determines which threshold(s) they will use with the model, regardless of the developer’s upstream validation.

In this way, a model user can create unfair outcomes through their choice of thresholds, even if the original model was relatively well calibrated and ostensibly fair. Even if the model user notices biased outcomes, the application of fairness interventions can be prohibitively data hungry or computationally expensive, and, in many cases, the model user may not have the expertise to retrain the model for their specific use case. All this to say, fair models are brittle: if they are used beyond the particular assumptions made at development time, their fair properties are weakened [49].

The core question which motivates our work, therefore, is as follows: how can we create a model that is fair irrespective of how it is used downstream? Specifically, we focus on settings where a model user has a correctly validated model from an upstream developer, but has a choice in threshold(s) for their specific domain. From this, we can formally restate our problem: **In the context of binary classification, how might we arrive at a model which produces fair decisions irrespective of the threshold used?** Our contributions are as follows.

- (1) We introduce a post-processing framework for achieving various (classification-based) definitions of fairness over all possible choices in threshold; provide theoretical justifications for our approach, and demonstrate how to use our method in the case where the sensitive attribute is binary.
- (2) We extend our framework to a setting where the protected attribute takes on more than two values and motivate the use of lexicographic fairness for our problem; show how to compute a lexicographically fair solution; and illustrate the connection to the simpler approach introduced for binary sensitive attributes.

In Section 1.1, we overview the problem setting in more detail. In Section 2, we provide technical background for our method and begin to show the connections between fairness and ideas from optimal transport. Section 3 details the key ideas of our proposed method, its theoretical justifications, and some experimental evidence validating our approach. In Section 4, we discuss the limitations of other methods for achieving fairness based on optimal transport. Then, in Section 5, we extend our approach to address settings where the protected attribute takes on more than two values and examine the effectiveness of our approach with a case study based on FICO credit scores. Finally, Section 6 discusses the implications and limitations of our approach as well as intended future work and open questions.

## 1.1 Notation & Setting

We begin by introducing the notation and framework we use for fair regression and *binary* classification. A notation glossary can be found in Appendix A.1. Allow  $\mathcal{G}$  to be the set of protected attributes. First, we consider the binary protected group setting  $\mathcal{G} = \{0, 1\}$ . Let  $D = \{(x_i, g_i, y_i)\}_{i=1}^N$  be a dataset consisting of features  $x_i \in \mathbb{R}^d$ , a protected attribute  $g_i \in \mathcal{G}$ , and a classification label  $y_i \in \{0, 1\}$ . Allow  $f : X \times \mathcal{G} \rightarrow \Omega$  with  $\Omega = [0, 1]$  to be a regressor that estimates the likelihood  $(x, g)$  attains the outcome denoted by the positive classification label

$$f(x, g) = \Pr(Y = 1 | X = x, G = g) \tag{1}$$

where  $X, G, Y$  are the associated random variables. We will often refer to the probabilities output by  $f(x, g)$  as *scores* given that they “rank” the  $(x, g)$  based on their estimated likelihood of attaining the outcome associated with  $Y = 1$ . The scores output from  $f(x, g)$  are used to determine discrete decisions denoted  $\hat{y} \in \{0, 1\}$ . For binary predictions, these are obtained using a threshold  $\tau \in [0, 1]$  where  $\hat{y}_i = \mathbb{1}_{f(x_i, g_i) \geq \tau}$ .

If a regressor performs poorly for one group, or if the base risk of two groups differs, classifications instantiated from thresholding can lead to unbalanced allocation of interventions across groups, and ultimately lead to disparate impact [15, 25, 43, 53].<sup>1</sup> If the thresholds used to produce classifications are known or assumed at model development time, there is a myriad of fair interventions which can be deployed to (at least partially) mitigate disparities [3, 12, 25, 39, 56] at deployment. There are many situations however, where classification thresholds are not known in advance, or may change over time. Consider a case where the model user lacks the expertise or resources to train a model. This frequently occurs in healthcare and criminal justice contexts, where predictive scores are used in tandem with human experts to allocate treatments or determine legal decisions [15, 47]. In these contexts, model users will operationalize the model at whichever threshold best suits their domain-specific requirements. We make this clear in the following example:

*EXAMPLE 1.1. Suppose a healthcare organization has a model to predict the likelihood of being diagnosed with severe illness. An outreach team may want to notify all the patients that are more likely than not to be diagnosed, therefore using a threshold of 0.5 to determine which patients to contact. The clinical team, on the other hand, only has the resources to treat the riskiest patients, and therefore uses a much higher threshold, such as 0.8, to determine which patients to treat.*

Ideally, a regressor performs well under some fairness metric regardless of the decision threshold that is selected. In practice, however, this is often not the case. In fact, it is well studied that different choices in threshold can lead to wildly different social outcomes [32, 37, 54]. From this observation, we see that fair solutions are often not portable [2]; achieving fairness with respect to one specific application or threshold does not imply fair performance at other thresholds [20] for a similar task or even for the same model. Moreover, if the use case or underlying population of a model change downstream, but retraining or modifying a model is not viable (e.g. is prohibitively expensive), additional engineering is required in order to ensure model performance. Our solution is to develop a model which is fair with respect to many thresholds *at the same time*. If a model can achieve fairness across *all* possible choices in threshold *simultaneously*, it can be deployed by any downstream user who flexibly utilizes such a model at different thresholds, and subsequently for different applications.

## 2 FAIR REGRESSORS & OPTIMAL TRANSPORT

In this section, we will overview important preliminaries in algorithmic fairness and optimal transport, and discuss the connection between the two. Then, we will introduce total and geometric repair, two techniques that lie at the intersection of fairness and optimal transport, and begin to motivate their use in our post-processing method.

### 2.1 Fairness Metrics and the Confusion Matrix

In the context of classification, the performance of a classifier<sup>2</sup> is often evaluated by performance metrics in the confusion matrix. For a regressor  $f$ , each of these confusion-matrix based metrics is a function  $\gamma_g^{y,c} : \Omega \rightarrow [0, 1]$  such that

$$\gamma_g^{y,c}(\tau) = \Pr[\hat{Y}(\tau) = c | Y = y, G = g] \quad (2)$$

where  $y, c \in \{0, 1\}$  denote dataset label and predicted class respectively, and  $g$  denotes protected attribute such that  $\Pr[\hat{Y}(\tau) = c | G = g] = \mathbb{E}_{x \sim X}[\mathbb{1}_{\hat{y}=c} | G = g]$  with  $\hat{y} = \mathbb{1}_{f(x,g) \geq \tau}$  indicating that  $\hat{y} \sim \hat{Y}$ . For a regressor  $f$ , we refer to the set of all such confusion-matrix based metrics  $\gamma_g^{y,c}(\tau)$  as  $\Gamma_f$ . For example, under this notation, the True Negative Rate

<sup>1</sup>Here, disparate impact does not refer to the 80/20 legal doctrine, nor the frequently referenced fairness criteria [25], but rather refers to each group observing different impacts from some machine learning tool. See [5] for a complete treatment of this discussion.

<sup>2</sup>Herein, “classifier” will refer to thresholded output of a regressor.

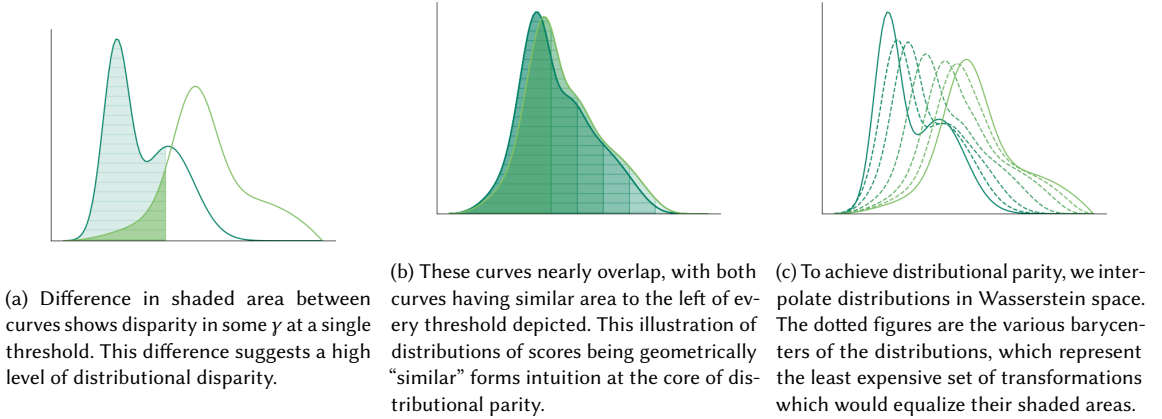


Fig. 1. An illustration of distributional parity and its relationship to the Wasserstein geometry of distributions. Each plot shows groupwise distributions of scores.

(TNR) of a classifier for some group  $g$  is  $\gamma_g^{0,0}(\cdot)$  (see Table 2 in the appendix for additional examples). In cases where we consider both values of a sub/superscript, we omit it from our  $\gamma$  notation. For example, the Positive Rate (PR) of the classifier is written  $\gamma^{c=1}(\cdot)$  since we consider all groups  $G = 0, 1$  and all labelings  $Y = 0, 1$ . Occasionally we may also index our metrics  $\gamma_k$ .<sup>3</sup>

Returning to our original goal, we’d like to express the fairness of some classifications across all thresholds, for  $\Gamma_f$ . To express exact equality in these metrics across all threshold we introduce the notion of distributional parity.

**DEFINITION 2.1 (DISTRIBUTIONAL PARITY).** A regressor  $f$  satisfies **distributional parity** with respect to  $\gamma \in \Gamma_f$  if

$$|\gamma_{g=1}^{y,c}(\tau) - \gamma_{g=0}^{y,c}(\tau)| = 0 \quad \forall \tau \in \Omega, y \in Y, c \in C. \quad (3)$$

with  $\mathbb{E}_{\tau \sim U(\Omega)} |\gamma_{g=1}^{y,c}(\tau) - \gamma_{g=0}^{y,c}(\tau)|$  acting as a measure of distributional (dis)parity.<sup>4</sup>

Definition 2.1 generalizes existing definitions of *strong* fairness. For example, if we were to consider only the Positive Rate of each group, we recover the definition of Strong Demographic Parity from Jiang et al. [38].

**DEFINITION 2.2 (STRONG DEMOGRAPHIC PARITY (SDP)).** A regressor  $f$  satisfies **strong demographic parity** if

$$\max_{\tau \in [0,1]} |\gamma_{g=1}^{c=1}(\tau) - \gamma_{g=0}^{c=1}(\tau)| = 0 \quad (4)$$

It has been shown that Strong Demographic Parity is closely related to notions of statistical distance, specifically the Wasserstein Distance [17, 28, 29, 38]. In the next section, we will briefly introduce the Wasserstein Distance and demonstrate its connection to SDP and other measures of distributional parity.

<sup>3</sup>Note although we do not address this case specifically, our framework can be easily extended to the  $m$ -multiclass setting by considering  $c_1, \dots, c_m$  and using rates of the form  $\gamma^{c=c_i}$  for positive classification of class  $c_i$  or  $\gamma^{c \neq c_i}$  in the negative case.

<sup>4</sup>We refer to “distributional parity” both as a fairness notion and as a fairness metric.

## 2.2 Wasserstein Preliminaries

Let  $p \geq 1$ , and  $\mathcal{P}_p(\Omega)$  be the space of Borel probability measures<sup>5</sup> on  $\Omega$  with finite  $p^{\text{th}}$  moments. We denote the distribution of scores for group  $g \in \mathcal{G}$  as  $\mu_g \in \mathcal{P}_p(\Omega)$ . The cumulative distribution function (CDF) of any  $\mu$  is denoted  $F_\mu(\tau) = \mu((-\infty, \tau])$ . We also make heavy use of the generalized inverse of the CDF of some  $\mu$ , called the quantile function, denoted  $F_\mu^{-1}$ . In cases where  $\text{supp}\mu \neq \Omega$ , the CDF of  $\mu$  is not strictly increasing, and therefore does not have a well defined inverse. In this case, we define the quantile function as a pseudo-inverse.

**DEFINITION 2.3 (PSEUDO-INVERSE OF A CDF).** *Given some cumulative distribution function  $F_\mu : \Omega \rightarrow [0, 1]$  its **pseudo-inverse** is the function  $F_\mu^{-1} : [0, 1] \rightarrow \Omega$  where  $F_\mu^{-1}(a) = \inf\{\tau \in \Omega : F_\mu(\tau) \geq a\}$*

**2.2.1 Wasserstein Distance.** The Wasserstein distance is a method of comparing two probability distributions by measuring the “cost” of transporting one distribution to another. If this transportation is costly, then the Wasserstein distance between the two distributions will be large. Formally, suppose  $\Omega_x, \Omega_y \subseteq \Omega$  are endowed with cost function  $c : \Omega_x \times \Omega_y \rightarrow \mathbb{R}$ . Let  $\mu \in \mathcal{P}_p(\Omega_x)$  and  $\nu \in \mathcal{P}_p(\Omega_y)$ . The notion of transport is formally defined by a **transport plan**. A transport plan is a function  $T : \Omega_x \rightarrow \Omega_y$  subject to the following constraint: if the elements in the pre-image of  $T$  have measure  $\mu$ , and the output of  $T$  is distributed according to  $\nu$ , i.e. if  $T$  is the transport plan from  $\mu \rightarrow \nu$  then  $\nu(A) = \mu(T^{-1}(A))$  for all measurable  $A \subseteq \Omega_y$ . The measure resulting from a transportation  $T$  plan from  $\mu \rightarrow \nu$  under this constraint is called the push forward of  $\mu$  and is denoted  $T_\# \mu = \nu$ . Let  $\mathcal{T}$  be the set of transportation plans. The *optimal* transport plan is the plan that obeys push-forward constraints while minimizing transportation costs

$$T^* := \arg \inf_{T \in \mathcal{T}} \int_{\Omega} c(\omega, T(\omega)) d\mu(\omega) \quad \text{where} \quad T_\# \mu = \nu. \quad (5)$$

For univariate measures, the optimal transport plan and Wasserstein distance both admit a closed form. The transport plan  $T$  from  $\mu \rightarrow \nu$  is computed  $T(\omega) = F_\nu^{-1}(F_\mu(\omega))$ , and the Wasserstein distance is computed as follows:

**DEFINITION 2.4 (WASSERSTEIN DISTANCE<sup>6</sup> ON UNIVARIATE MEASURES).**

$$\mathcal{W}(\mu, \nu)_p^p := \left( \int_{\Omega} |F_\mu^{-1}(x) - F_\nu^{-1}(x)|^p dx \right) = \|F_\mu^{-1} - F_\nu^{-1}\|_{L_p(\Omega)}^p. \quad (6)$$

From the second equality, we can also see that the geometry of univariate probability measures in Wasserstein space is linear-like,<sup>7</sup> allowing us to evoke familiar geometric concepts like midpoints, or averages, but over probability measures and using the Wasserstein distance as a distance kernel.

**2.2.2 Wasserstein Barycenters.** The midpoint or geometric average of a set of measures in Wasserstein space is called the Wasserstein Barycenter [4]. Intuitively, the barycenter is a weighted composition of several probability measures, geometrically averaging their densities into a single new probability measure.

**DEFINITION 2.5 (WASSERSTEIN BARYCENTER).** *Allow  $\mu_1 \dots \mu_m \in \mathcal{P}_p(\Omega)$  and  $\vec{w} \in \mathbb{R}^m$  to be a weight vector with  $\sum_{i=1}^m w_i = 1$ . The **Wasserstein Barycenter** of these measures, denoted by  $\beta$  is*

$$\beta := \arg \min_{\nu \in \mathcal{P}_p(\Omega)} \sum_{i=1}^m w_i \mathcal{W}_p(\nu, \mu_i). \quad (7)$$

<sup>5</sup>We review the atomicity of these distributions in the Appendix A.3

<sup>6</sup>Wasserstein distances on  $\mathbb{R}$  are sometimes referred to as Earth Mover distances.

<sup>7</sup>The map  $\mu \rightarrow F_\mu^{-1}$  is an isometric embedding which can map the Wasserstein space defined  $(\mathcal{P}_p(\Omega), \mathcal{W}_p(\cdot, \cdot))$  to the space  $L_p(\Omega)$ .

### 2.3 On the Connection between Wasserstein Distance and Fairness Metrics

There is an intimate connection between fairness metrics in  $\Gamma_f$  and the Wasserstein distance. Specifically, the average difference (taken over thresholds) in some performance metric across groups is measured by the Wasserstein distance between the score distributions of each group. We express this formally with Proposition 2.6.

**PROPOSITION 2.6.** *Let  $f : X \times \mathcal{G} \rightarrow \Omega$  and assume without loss of generality that  $c = 1$ . Then, let  $\mu_{g=0}^y, \mu_{g=1}^y$  be the groupwise distributions of scores  $f$  produces. We have*

$$\mathbb{E}_{\tau \in U(\Omega)} |\gamma_{g=1}^y(\tau) - \gamma_{g=0}^y(\tau)|^p = \mathcal{W}_p^p(\mu_{g=0}^y, \mu_{g=1}^y). \quad (8)$$

*Proofs of mathematical results can be found in Appendix E.*

If we consider  $\gamma_g^{c=1}$ , then the first term in Proposition 2.6 measures distributional disparity with respect to positive rates, functioning like a disparity metric for strong demographic parity. Results from [17, 28, 29, 38] have already shown that achieving strong demographic parity is equivalent to vanishing the Wasserstein distance between group-conditioned score distributions. With the above proposition, we extend this result to all rates in the confusion matrix.

Although this is a handy result, what remains to show is a *good* way of removing the Wasserstein distance between some group-conditional distributions: *how do we modify a regressor such that the Wasserstein distance between its group conditioned score distributions is minimized?* So far, this has been achieved using total and geometric repair. Next, we will introduce these repair methods and demonstrate their use.

### 2.4 Geometric Repair and Fair Regressors

One way to eliminate the Wasserstein distance between some distributions is to map them onto some common distribution such that for each group, all scores are *distributed identically* under the image of this mapping. The Wasserstein barycenter is a candidate distribution in this regard due to several optimal properties. Notably, Jiang et al. [38] show that transport onto the 1-Wasserstein barycenter *minimizes* changes to the predicted class<sup>8</sup> in pursuit of SDP. Similarly, Chiappa et al. [13] show that transport onto a Wasserstein barycenter is Pareto-optimal with respect to a tradeoff between fairness and accuracy. We will informally revisit this result in Section 3.1. In fact, the barycenter of univariate distributions can be computed as a closed-form solution to the optimization in Definition 2.5.

**REMARK 2.7.** *Given two distributions  $\mu, \nu \in \mathcal{P}_p(\Omega)$  and some  $w \in [0, 1]$ , the quantile function of their weighted barycenter is*

$$F_\beta^{-1}(q) = (1 - w)F_\mu^{-1}(q) + wF_\nu^{-1}(q), \quad q \in [0, 1] \quad (9)$$

*where  $\beta$  is the barycenter solution given in Definition 2.5.*

By applying Remark 2.7 for transport on univariate measures, we can compute a closed-form solution for the distribution-specific transportation functions that map from  $\mu$  or  $\nu$  onto their barycenter.

**COROLLARY 2.8.** *Recall that given two distributions  $\mu, \nu \in \mathcal{P}_p(\Omega)$  and their barycenter  $\beta$ , the optimal transport plan from  $\mu \rightarrow \beta$  is  $T_\mu(x) = F_\beta^{-1}(F_\mu(x))$  and from  $\nu \rightarrow \beta$  is  $T_\nu(x) = F_\beta^{-1}(F_\nu(x))$ . Suppose we allow the input to the quantile function of a barycenter be  $q = F_\mu(x)$ , then we can view the barycenter computation as the weighted sum of transportation*

<sup>8</sup>In fact, the expected changes in predicted class through total repair is exactly the quantity  $\mathcal{W}_1(\mu, \beta)$ . By Jensen's inequality we see  $\mathcal{W}_p(\mu, \beta) \leq \mathcal{W}_r(\mu, \beta)$  for all  $r \geq p \geq 1$  and so we assert this result holds for all orders of Wasserstein Distance.

plans

$$F_{\beta}^{-1}(F_{\mu}(x)) = (1 - w)F_{\mu}^{-1}(F_{\mu}(x)) + wF_{\nu}^{-1}(F_{\mu}(x))$$

If  $f(X, g) \sim \beta$  for both groups, then surely the Wasserstein distance between these group conditional score distributions  $\mathcal{W}(\mu_g, \mu_{g'}) = 0$ . With Proposition 2.6, we conclude that transporting scores onto their barycenter achieves distributional parity in a regressor. Like [16, 29], we can present a closed-form solution to this regressor.

**PROPOSITION 2.9.** *Let  $f : X \times \mathcal{G} \rightarrow \Omega$  be a regressor and define  $\alpha(x, g) = \inf\{a \in \Omega : F_{\mu_g}(a) \geq F_{\mu_{g'}}(f(a, g))\}$  for  $g, g' \in \mathcal{G}$ . With respect to some fair metric  $\gamma_g^y(\tau)$  their fair regressor  $f_{\beta} : X \times \mathcal{G} \rightarrow \Omega$  is*

$$f_{\beta}(x, g) = p_g f(x, g) + (1 - p_g) \alpha(x, g), \quad x \in X_y \quad (10)$$

where  $p_g$  is the likelihood of belonging to group  $g$  and  $X_y$  is the set of all elements with labeling  $y$ .

This type of mapping to the barycenter for some fixed  $p$  is called *total repair* [25, 28]. These works also show that *partially* repairing some distributions by parametrizing the weights of the barycenter computation can be useful in computing a repair distribution. This type of repair is typically referred to as *geometric repair*, and is the basis for our main contributions.

### 3 DISTRIBUTIONAL FAIRNESS VIA GEOMETRIC REPAIR

Our key methodological contribution makes use of *geometric repair* to achieve distributional parity. Geometric repair is a type of partial repair which does not fully map distributions onto the barycenter, but rather linearly interpolates between the source distributions and their barycenter in Wasserstein space. Let's define the shift function  $t : X \times \mathcal{G} \rightarrow \Omega$ , which gives the difference between an unrepaired score and its fully repaired version:  $t(x, g) = f_{\beta}(x, g) - f(x, g)$ .

**DEFINITION 3.1 (GEOMETRIC REPAIR).** *Let  $\lambda \in [0, 1]$  be the **repair parameter**. We define *geometric repair* as*

$$f_{\beta}^{\lambda}(x, g) = f(x, g) + \lambda t(x, g) \quad (11)$$

Figure 2 illustrates our method on an example dataset (see Appendix B.1 for experimental details). The plots visualize various confusion matrix rates over all possible classifier thresholds, for each of two groups. When the group-conditional metric curves do not overlap, the resulting classifications will exhibit disparity; distributional parity is achieved only when the group-conditional metric curves overlap across all possible thresholds. In this example, while there is disparity over all thresholds in all three metrics displayed for the uncorrected score distribution ( $\lambda = 0$ ), various values of  $\lambda$  make it possible to achieve distributional parity in positive rates, true positive rates, and false positive rates. This is an empirical illustration of the following observation: with a single barycenter, for *any* distributional parity metric in  $\Gamma_f$ , there is always a value for the repair parameter  $\lambda$  which minimizes that metric – through mapping onto the  $\lambda$ -repaired distribution. We explain this result by examining some key properties of geometric repair and Wasserstein space.

#### 3.1 Wasserstein Geodesics

Geometric repair is a method for optimally interpolating between distributions in Wasserstein space. Here, optimal refers to the length of the “path” that emerges between two measures and their barycenters for various values of the weight parameter  $\lambda$ . This path is called a geodesic, and it defines a length-minimizing path between distributions in Wasserstein space.

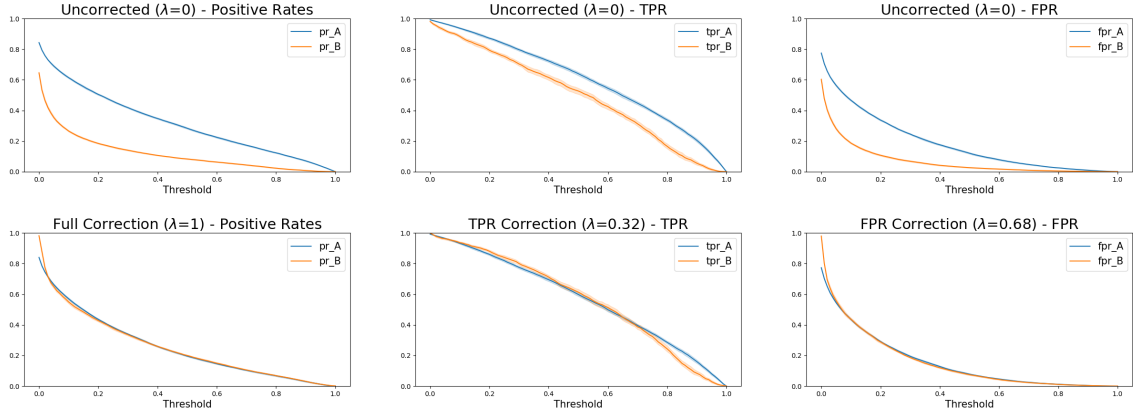


Fig. 2. Experiments using the (old) Adult dataset. X-axis: all possible choices of threshold  $\tau \in [0, 1]$ . Y-axis: group-conditional selection rate, TPR, and FPR for the classifications resulting from each possible  $\tau$ . Top row: classifications based on original, uncorrected classifier probabilities. Bottom left: full correction ( $\lambda = 1$ ). Bottom middle & right:  $\lambda \approx 0.32$ ,  $\lambda \approx 0.68$ .  $\lambda$  values are calculated based on the labelled training data, and shown here applied to the unlabelled testing data.

**DEFINITION 3.2 (WASSERSTEIN GEODESIC).** A curve  $\eta : [0, 1] \rightarrow \mathcal{P}_p(\Omega)$  is a **Wasserstein geodesic**<sup>9</sup> if for any  $\mu_0, \mu_1 \in \mathcal{P}_p(\Omega)$ , it locally minimizes the distance between any points along a curve between  $\mu_0, \mu_1$  with  $\eta(0) = \mu_0$  and  $\eta(1) = \mu_1$  such that  $\mathcal{W}_p(\eta(\lambda_1), \eta(\lambda_2)) = |\lambda_2 - \lambda_1| \mathcal{W}_p(\mu_0, \mu_1)$  for all  $\lambda_1, \lambda_2 \in [0, 1]$ .

**OBSERVATION 3.3.** Let  $\beta_\lambda$  be a set of measures between  $\mu_g, \mu_{g'}$  in Wasserstein space defined  $\beta_\lambda = \{v^* \in \mathcal{P}_p(\Omega) : v^* = \arg \min_{v \in \mathcal{P}_p(\Omega)} (1 - \lambda) \mathcal{W}_p(\mu_g, v) + \lambda \mathcal{W}_p(v, \mu_{g'}) \forall \lambda \in [0, 1]\}$ . Then,  $\beta_\lambda$  is the set of all barycenters between  $\mu_g$  and  $\mu_{g'}$  and contains all distributions along the geodesic [4].

This result indicates that geometric repair enumerates a geodesic of barycenters between distributions, and is therefore the *optimal* way to transport two distributions in Wasserstein space. In other words, given some desired amount of repair towards a fairness objective, geometric repair induces minimal changes to the original distributions, and therefore incurs minimal loss of their desirable properties. This suggests that geometric repair is optimal with respect to the infamous “fairness-utility trade-off,” as discussed in Section 2.1<sup>10</sup>.

With the following corollary, we show that geometric repair, as parametrized by  $\lambda$ , is able to recover every barycenter between two distributions: in other words, it can fully express the entire geodesic between curves through interpolation.

**COROLLARY 3.4.** A geometrically repaired regressor  $f_p^\lambda$  can be computed as the barycenter of  $\mu_g, \mu_{g'}$  with weights  $(1 - \lambda + \lambda p_g)$  and  $\lambda(1 - p_g)$ .

### 3.2 Optimization with the Barycenter: finding $\lambda$

We first show that for any metric  $\gamma \in \Gamma_f$ , there exists a value of  $\lambda \in [0, 1]$  that minimizes distributional disparity in the partially-repaired scores. Using Proposition 3.6, we will prove that metrics in  $\Gamma_f$  are convex on Wasserstein geodesics. This allows us to use standard optimization tools to find the value of the repair parameter  $\lambda$  that minimizes an objective function—specifically, distributional parity between two groupwise score distributions.

<sup>9</sup>This is also known as a constant speed geodesic.

<sup>10</sup>Despite these properties, there is extensive work criticizing and contesting the merit of the fairness-accuracy trade-off [18, 23].



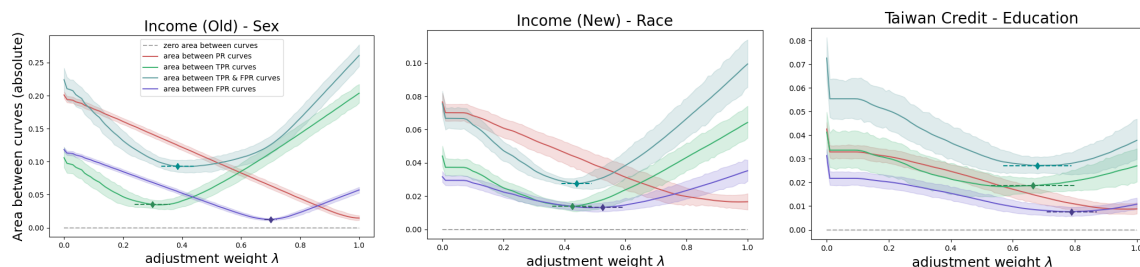


Fig. 3. Each plot shows the absolute (total) area between the pairs of curves belonging to  $\gamma_g, \gamma_{g'}$  after partial repair over possible values of  $\lambda \in [0, 1]$ . The diamond marker and dashed line indicate the average and 95% confidence interval for the value of  $\lambda$  which minimizes the area between the group-conditional curves for each metric.

First, we present Lemma 3.5, which motivates the convexity of distributional parity metrics. We begin by demonstrating that with respect to some metric  $\gamma$ , fair performance changes monotonically with the repair parameter. The direction of this change depends on which distribution has better average performance with respect to the desired metric—said differently, changes in the repair parameter will either strictly increase or decrease the value of a performance metric (e.g. true positive rate) at a given threshold. Allow  $\mu_g^\lambda$  to be the groupwise distribution of scores corresponding to the  $\lambda$ -repaired regressor, i.e.  $f_\beta^\lambda(x, g) \sim \mu_g^\lambda$ .

**LEMMA 3.5.** Fix some threshold  $\tau \in \Omega$ . Assume  $F_{\mu_g^\lambda}, F_{\mu_{g'}^\lambda}$  have continuous first derivatives for all  $\lambda \in [0, 1]$ . If  $F_{\mu_g^\lambda}(\tau) \geq F_{\mu_{g'}^\lambda}(\tau)$  then  $\gamma_g(\tau)$  decreases monotonically at that threshold with increase in  $\lambda$ , and increases monotonically if  $F_{\mu_g^\lambda}(\tau) \leq F_{\mu_{g'}^\lambda}(\tau)$ .

If at every threshold, one group’s distribution is monotonically “increasing” with respect to some metric during repair while the other’s is monotonically “decreasing,” it follows that the difference between the metrics should resemble a convex function, as both distributions move towards their barycenter with increases in  $\lambda$ . We formalize this intuition in the following theorem:

**THEOREM 3.6.** Define  $\delta_{\gamma_g}(\lambda) := \mathcal{W}_p^p(\mu_g^\lambda, \mu_{g'}^\lambda)$  or equivalently  $\delta_{\gamma_g}(\lambda) := \mathbb{E}_{\tau \in U(\Omega)} |y_g(\tau) - y_{g'}(\tau)|^p$  for all  $\lambda \in [0, 1]$  and  $\gamma_g \in \Gamma_{f_\beta^\lambda}$ . Then  $\delta_{\gamma_g}(\lambda)$  is convex.

**COROLLARY 3.7.** Let  $v \in \mathbb{R}_{\geq 0}^k$  and  $\gamma_{k=1} \dots \gamma_{k=k} \in \Gamma_f$ . The linear combination  $v_1 \delta_{\gamma_1}(\lambda) + \dots + v_k \delta_{\gamma_k}(\lambda)$  is also convex.

The convexity of  $\delta_\gamma$  implies that there exists a value of the repair parameter  $\lambda$  along the Wasserstein geodesic which can minimize groupwise differences in distributional parity. Additionally, Corollary 3.7, guarantees that a minima exists for any linear combination of metrics, thereby allowing us to compute a repair parameter that minimizes distributional disparity for multiple rates at once—for example, equalized odds, which measures both TPR and FPR differences.

Due to the convexity of distributional parity metrics, this repair parameter is guaranteed to achieve a minima<sup>11</sup>, and is computed by solving the following optimization<sup>12</sup>.

<sup>11</sup>This minima is only guaranteed to be locally optimal; we aim to characterize the global optimality of this approach in future work.

<sup>12</sup>The optimal repair parameter for any distributional parity metric can be calculated exactly using standard convex optimization tools

REMARK 3.8. Let  $f_{\beta}^{\lambda}(x, g)$  be a repaired regressor,  $\gamma_{k=1 \dots \gamma_{k=k}}$  be performance metrics in  $\Gamma_{f_{\beta}^{\lambda}}$  and  $\vec{w} \in \mathbb{R}_{\geq 0}^k$  be a weight vector, the distributional parity minimizing  $\lambda^*$  along the geodesic<sup>13</sup> is given by

$$\lambda^* \leftarrow \arg \min_{\lambda \in [0,1]} \sum_{j=1}^k w_j \mathbb{E}_{\tau \in U(\Omega)} [\gamma_{k=j,g}(\tau) - \gamma_{k=j,g'}(\tau)] \quad (12)$$

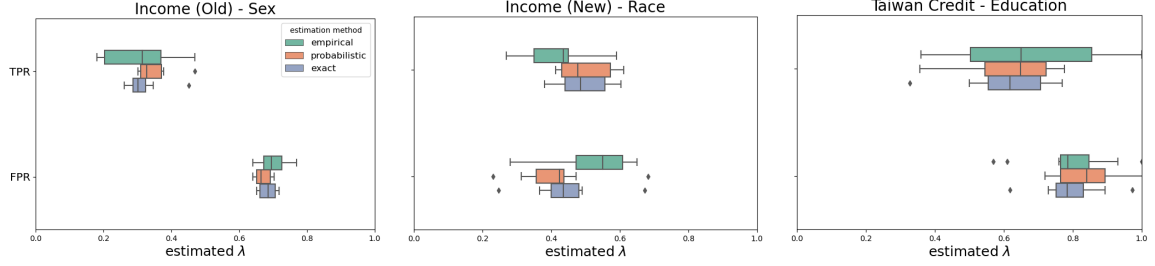


Fig. 4. A comparison of three methods of finding  $\lambda$ s: empirical estimation, which was done by testing all values of  $\lambda$ , probabilistic estimation, which was calculated according to Proposition 3.10, and exact calculation, as in Remark 3.8, over the same ten trials.

### 3.3 Estimating $\lambda$ with Probabilistic Distributional Parity.

As datasets become large, computing the distributional (dis)parity minimizing  $\lambda$  in Remark 3.8 can become computationally expensive, as the objective function must evaluate some  $\gamma$  across the entire dataset, and at every threshold. Although this computation is not always prohibitively expensive, in more complex optimization routines like that of Section 5, it can become extremely slow in practice. To remedy this issue, we present a high-quality approximation for such an optimal  $\lambda$ . The exact value of  $\lambda$  that minimizes a distributional parity metric can be approximated instantaneously with Probabilistic Distributional Parity, an extension of probabilistic equal opportunity as introduced in Taskesen et al. [50].

DEFINITION 3.9 (PROBABILISTIC DISTRIBUTIONAL PARITY). A regressor  $f$  satisfies **Probabilistic Distributional Parity** if

$$\mathbb{E}_{x \sim \mathcal{X}_g} [f(x, g) | Y = y, G = g] = \mathbb{E}_{x \sim \mathcal{X}_{g'}} [f(x, g) | Y = y, G = g']. \quad (13)$$

Like its non-probabilistic counterpart, Probabilistic Distributional Parity encompasses all metrics contained in  $\Gamma_f$ . For example, to consider a probabilistic variant of equal opportunity, we compute the above expectation with  $Y = 1$ ; conversely, for false positive rates, we condition on  $Y = 0$ . Computing a repair parameter with respect to probabilistic distributional parity also admits a closed form solution.

PROPOSITION 3.10. The  $\lambda$  which approximates the optimal repair parameter with respect to some fairness definition is

$$\lambda = \frac{\mathbb{E}_{\mathcal{X}_{g'}} [f(x, g') | Y, G = g'] - \mathbb{E}_{\mathcal{X}_g} [f(x, g) | Y, G = g]}{\mathbb{E}_{\mathcal{X}_g} [t(x, g) | Y, G = g] - \mathbb{E}_{\mathcal{X}_{g'}} [t(x, g') | Y, G = g']} \quad (14)$$

In Figure 4, we illustrate the quality of  $\lambda$  approximations using Proposition 3.10. In addition to  $\lambda$ 's computed with exact and probabilistic methods, we also show the empirical  $\lambda$  found in each trial<sup>14</sup>. Note the range of estimated optimal  $\lambda$ s is remarkably similar for both methods across all ten random splits of the dataset.

<sup>13</sup>We refer the reader to Algorithm 2 in the appendix to compute this exactly.

<sup>14</sup>See Appendix B.1 for experimental details.

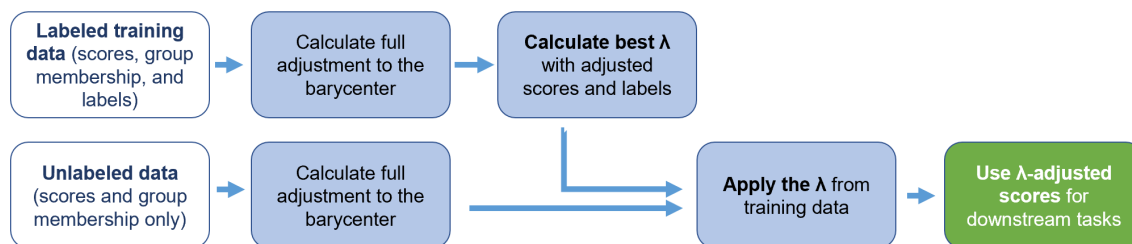


Fig. 5. A summary of how each step of our post-processing method proceeds. As noted in [17], calculating the adjustment of score distributions to the barycenter does not require ground-truth labels. Labels are only required to determine the best  $\lambda$  for the dataset given a desired metric;  $\lambda$ s are therefore calculated with the labeled training data and are used to control the barycenter adjustment for unlabeled data. Finally, note that we do not require any of the features used for the machine learning model, only group membership and the model’s predicted scores. This general framework also describes our method workflow for the setting discussed in Section 5.

Finally, we are ready to summarize our general approach, illustrated in Figure 5. Appendix D provides additional comments on using our method in practice.

#### 4 LIMITATIONS OF EXISTING METHODS

Our approach is most closely related to other works using optimal transport to satisfy notions of fairness. In [17, 29, 38], optimal transport is used to achieve strong demographic parity; however, these works do not extend their approach to other metrics in the confusion matrix. In [25, 28] optimal transport is applied to the input features, whereas our work focuses on applying optimal transport to classifier output. In addition, the quality of Wasserstein distance estimation in optimal transport decreases in higher dimensions (i.e. on input features), whereas using only output scores, we do not suffer the same curse-of-dimensionality issues [14]. A growing body of work utilizes the Wasserstein distance as a measure for fairness, achieving fair classification through distributionally robust optimization [50, 52]; however, these works are a train-time intervention, rather than post-processing.

Our problem setting is conceptually similar to the problem of fair regression [7, 16, 17], where the goal is to achieve some definition of fairness by adjusting the group-conditional distribution of predictions in a continuous output space. However, we do not seek to make groupwise distributions *identical*; this also distinguishes our work from the fair top- $k$  ranking problem [55]. Vogel et al. [51] also explore the problem of adjusting rankings in order to satisfy classification fairness for many thresholds; however, they propose an in-processing method for *learning* the scores during train time.

As a fairness intervention, our work is most closely related to other post-processing methods such as those implemented in popular libraries like IBM’s AI Fairness 360 [6], Microsoft’s Fairlearn [8], or those introduced in [32, 40, 48]. In these works, fair classifications are produced over some discrete decision space, thereby implying a *specific* decision threshold, and limiting their applicability in the upstream/downstream case we study here. The post-processing method introduced by Kim et al. [42] seeks to achieve *multiaccuracy*, i.e. equally-accurate predictions across all identifiable subgroups of the data. Hébert-Johnson et al. [33], which seeks *multicalibration*, requires building a model from scratch.

Our method is an improvement on these approaches for several reasons: first, it is a *post-processing* method and can therefore make use of information learned by an existing classifier; second, our approach can achieve multiple definitions of distributional parity; and third, as we will detail below, our approach can naturally accommodate a sensitive attribute which takes on more than two attributes. Though many of the works described above satisfy one or multiple of these qualities, ours is the only to our knowledge that satisfies all three.

## 5 BEYOND BINARY PROTECTED ATTRIBUTES

In cases where a protected attribute takes on more than two values (i.e. where  $|\mathcal{G}| \geq 2$ ), the problem of locating an optimal repair parameter becomes more complex. In the binary attribute setting, there was only one possible comparison to optimize. In the non-binary attribute setting, however, the number of possible pairwise comparisons between groups is exactly  $\binom{|\mathcal{G}|}{2}$ , which grows quadratically as the number of groups increases. Now, suppose instead there are  $n$  protected groups such that  $g = \{g_1, \dots, g_n\}$ . As a necessary consequence of this extension, we introduce repair parameters for each group  $1 \leq i \leq n$

$$f_{\beta}^{\lambda_i}(x, g_i) = f(x, g_i) + \lambda_i t(x, g_i). \quad (15)$$

Achieving distributional parity in *positive rates* in this context remains the same: we solve this with total repair, by mapping each group’s score distribution completely onto a barycenter, by setting  $\lambda_i = 1$  for all  $i \in [n]$ . Achieving other notions of distributional parity, however, is complicated by the fact we are searching for some optimal repair *vector*  $\vec{\lambda} = (\lambda_1 \dots \lambda_n)$  in an  $n$ -dimensional space. This higher dimensional search problem introduces additional challenges. In general, a fair intervention which minimizes disparities in a performance metric across all groups simultaneously can artificially benefit or disadvantage some groups with respect to that metric [20, 37]. In the binary sensitive attribute setting, *max-min* fairness was introduced to alleviate this tension [44]: a max-min solution maximizes the performance of the group that is worst off without minimizing the performance of the other, presumably advantaged, group. One common criticism of current fair algorithmic scholarship, however, is that binary protected attributes are not expressive enough to create a meaningful model for the study or design of fair interventions that work in practice [11, 31, 35, 41].

As we look to extend geometric repair to the non-binary attribute setting, max-min fairness is no longer sufficient, since the formulation of max-min fairness relies on the assumption that protected attributes are binary. Suppose we wish to achieve a max-min-like solution for an protected attribute that takes on multiple (non-binary) values. Although a learning problem can be constrained to replicate a max-min-like solution for all groups, this requires the practitioner to develop a complete ordering of disparities—in other words, to explicitly identify the group which should have the highest performance, the group which should have the second highest performance, and so on. For a large protected attribute space, this task requires a rather large normative judgement on behalf of the practitioner. Even if this ordering were to exist, it still has the potential to decrease overall groupwise performance, due to performance tradeoffs that may be associated with the prescribed ordering of disparities [41]. *Lexicographic fairness* was proposed to remedy the above concerns. Here, we will describe lexicographic fairness as introduced to the supervised learning literature, detail its relevance to geometric repair, provide a constrained optimization algorithm that outputs a lexicographically fair repair vector, and finally conclude with a case study on FICO credit scores.

### 5.1 Lexicographic Fairness

Lexicographic fairness, introduced to the learning literature by Diana et al. [21] as an adaptation of previous work from social choice and fair division [10, 36], is an extension of max-min fairness [44] that minimizes group-conditional error rates in a way that prioritizes the groups that are the worst off. More specifically, a lexicographically fair approach will first minimize the loss of the worst off group, and then use the loss under of the worst off group as a constraint to minimize the loss of the next worst off group, continuing until all groups have had their losses minimized subject to the constraints established by minimizing the losses for better-off groups.

Allow  $\mathcal{H}$  to be the space of hypothesis for the classification task. Let  $L_g : \mathcal{H} \rightarrow \mathbb{R}$  be the loss for the group defined  $g$ . We define the total loss of a hypothesis as the sum of group loss terms:

$$L(h) = \sum_{i=1}^n a_{g_i} L_{g_i}(h) \quad (16)$$

where  $a_{g_i} \in \mathbb{R}_+$  represents the weight given to the loss term corresponding to group  $g_i$ . Allow  $\mathcal{O} : [n] \rightarrow \mathcal{G}$  to be a bijection ordering the group error rates in decreasing order such that  $L_{\mathcal{O}(1)}(h) > L_{\mathcal{O}(2)}(h) \dots > L_{\mathcal{O}(n)}(h)$ . The total error rate for some hypothesis is computed recursively and in rounds. At the  $k^{\text{th}}$  round where  $1 \leq k \leq |\mathcal{G}|$ , the error rate is defined  $\epsilon_k := \min_{h \in \mathcal{H}_{k-1}} L_{\mathcal{O}(k)}(h)$  where  $\mathcal{H}_{k-1}$  is the hypothesis class at  $k^{\text{th}}$  round constrained to the set of hypotheses which minimized at the previous rounds  $H_k = \{h \in H_{k-1} : L_{\mathcal{O}(k)}(h) \leq \epsilon_k\}$ <sup>15</sup>. A lexicographically fair solution is one which achieves the error rates defined recursively in this way.

**DEFINITION 5.1 (LEXICOGRAPHIC FAIRNESS).** *A model  $h \in H$  satisfies lexicographic fairness if  $L_{\mathcal{O}(k)}(h) \leq \epsilon_k$  for all  $k \leq n$ .*

Note that max-min fairness is actually a special case of lexicographic fairness. That is, a max-min solution is identical to a single round of lexicographic optimization; see Appendix C.1 for more detail.

Because lexicographic fairness is defined recursively, the set of hypotheses that satisfy the above definition is not convex. To make lexicographic fairness a convex set, we redefine the space of lexicographically fair hypotheses by enumerating the recursive constraints into many linear constraints:

**DEFINITION 5.2 (CONVEX LEXICOGRAPHIC FAIRNESS).** *A model  $h$  satisfies convex lexicographic fairness if*

$$\max_{R \in 2^{\mathcal{G}}, |R| \leq j} \sum_{g \in R} L_{\mathcal{O}(i)}(h) \leq \min_{h' \in \mathcal{H}_{j-1}} \max_{R \in 2^{\mathcal{G}}, |R| \leq j} \sum_{g \in R} L_g(h') \quad \forall k \leq n, j \leq k. \quad (17)$$

Diana et al. [21] show that a convex lexicographically fair classifier has the same error profile as its non-convex counterpart, and that if the original model class  $\mathcal{H}$  is convex, then the lexicographically fair subset of hypothesis that satisfy the above definition will also be convex.

## 5.2 Achieving Distributional Parity with Lexicographic Fairness

To apply the lexicographic fairness approach to our setting, we use Probabilistic Distributional Parity, defined in Section 3.1, as the group loss function:

$$L_{g_i}(\vec{\lambda}) = \sum_{j \leq n, i \neq j} |\mathbb{E}_{X_{g_i}|Y}[f(x, g_i)] - \mathbb{E}_{X_{g_j}|Y}[f(x, g_j)]| \quad (18)$$

Due to the convexity of Probabilistic Distributional Parity, this loss is also convex. Allow  $\Lambda_\ell \subseteq \mathbb{R}^n$  to be the set of lexicographically fair repair parameters. We compute the lexicographically fair repair as the solution to the following optimization, subject to the constraint set at round  $k \leq n$ :

$$\min_{\vec{\lambda} \in \Lambda_\ell} \sum_{i=1}^n L_{g_i}(h, \vec{\lambda}) \quad \text{s.t.} \quad C_k(\epsilon_1 \dots \epsilon_k) = \left\{ \sum_{i_j} L_{i_j} \leq \epsilon_j : (i_1, \dots, i_j) \subseteq [I] \quad \forall j \leq k \right\}. \quad (19)$$

We present full pseudo-code for this procedure, formalized as Algorithm 3, in Appendix C.1, and summarize the intuition here. At the first round ( $k = 1$ ), the algorithm computes a max-min fairness solution by minimizing loss for

<sup>15</sup>Note  $k$  is slightly overloaded—our use of  $k$  here, to index rounds of lexicographic optimization, is different from its usage in Section 3.

the group that is worst off. The worst loss in the max-min solution is  $\epsilon_1$ . At the second round ( $k = 2$ ), the algorithm minimizes the loss of the second worst-off group, subject to the condition that no single group’s loss may exceed the loss of the max-min solution  $\epsilon_1$ . Then, the loss of the two worst off groups under the max-min solution becomes  $\epsilon_2$ . At the third round ( $k = 3$ ), the algorithm minimizes the loss of the third worst-off group, subject to the constraint that no two groups have a combined loss greater than  $\epsilon_2$ , and that no single group has a loss which exceeds  $\epsilon_1$ . The algorithm continues in this fashion until the last round, where the final lexicographic solution  $\lambda_k$  is computed. Next, we show in Theorem 5.3 that Algorithm 3 outputs a lexicographically fair solution for some probabilistic distributional parity loss.

**THEOREM 5.3.** *For a convex and bounded choice in loss function  $L : \mathbb{R}^n \rightarrow \mathbb{R}$  and convex hypothesis class  $\mathcal{H}$ , Algorithm 3 will output a lexicographically fair solution.*

### 5.3 Case Study: FICO

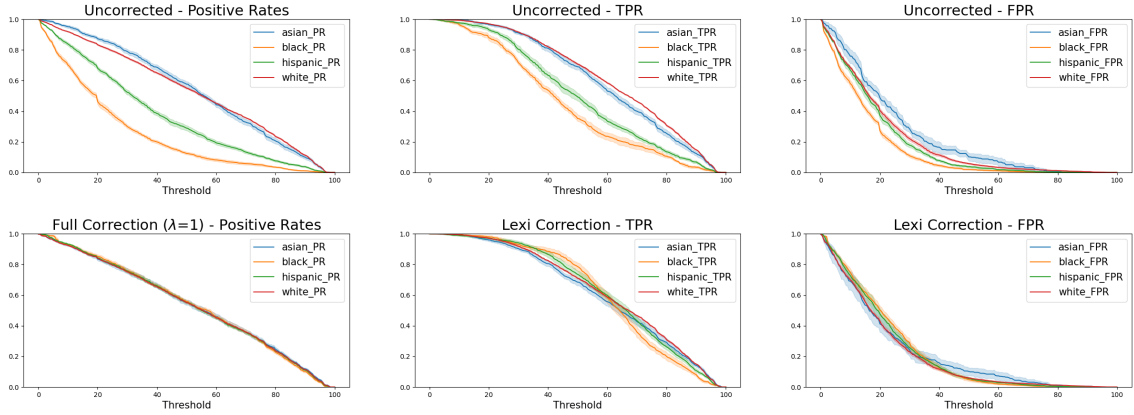


Fig. 6. A replication of Figure 2, now with a sensitive attribute that takes on four values using the FICO dataset. X-axis: all possible choices of threshold  $\tau \in [0, 100]$ . Y-axis: group-conditional positive rate, TPR, and FPR for the classifications resulting from each  $\tau$ . Top row: classifications based on uncorrected scores. Bottom row: classifications based on  $\lambda$ s calculated with Algorithm 3.

To demonstrate the effect of our proposed post-processing, we study various repair methods on FICO credit scores. The goal of a credit score is to estimate an individual’s general credit risk, where low scores should correspond to high-risk individuals and high scores to low-risk individuals. In the United States, credit scores for various minority groups are often lower than those of their white counterparts despite similar monetary behaviors and financial histories [46]. The FICO credit scores we examine are sourced from a 2003 government report that collected TransUnion credit data on  $\sim 300k$  individuals. The dataset consists of an individual’s ethnic group (which we use as a protected group), their credit score, and an outcome label  $Y$  where  $Y = 0$  if an individual failed to pay a debt within 18–24 months of the data being collected.<sup>16</sup> We can consider the credit scores to be the output of an unknown regressor  $f$ .

Since credit scores are not equally representative of true creditworthiness for each group, any choice in threshold will induce some systematic disparity in access to credit when credit scores are relied upon as an accurate proxy for creditworthiness. Consider an algorithm developer who highly values identifying eligible borrowers across groups, and suffers a high cost for missed lending opportunities. In this framework, the goal of the designer is TPR balance,

<sup>16</sup>Our FICO results also indicates our method’s flexibility—we do not require that the quantity being thresholded represents a probability.

otherwise known as equal opportunity. On the other hand, an algorithm developer who cares more about the cost of unpaid loans may seek to achieve FPR balance. Either way, we assume the developer is unsure which decision threshold will be used downstream, and wishes to produce a regressor which is fair regardless of choice in classification threshold. In this case study, to achieve TPR balance, we use probabilistic distributional parity loss with true positive rates, or probabilistic equal opportunity i.e.  $\mathbb{E}_{x \sim X}[f(x, g)|Y = 1, G = g]$  where  $X$  is the set of credit features used by the regressor. To achieve FPR balance, the loss function we use can be written as  $\mathbb{E}_{x \sim X}[f(x, g)|Y = 0, G = g]$ .

Figure 6 illustrates the efficacy of our method. While the uncorrected credit scores lead to substantial disparity in positive rates, true positive rates, and false positive rates across all thresholds, our method is able to find sets of  $\lambda$ s for each metric such that disparity is minimized across all thresholds. In each case, parity is achieved by improving performance on the worst-off groups, rather than worsening overall performance; this is especially clear in the TPR case (bottom middle). Additionally, note that unlike Figure 2, which illustrated the binary case, there is a *set* of  $\lambda$ s (one for each group) that achieves distributional parity in true positive rates, and a separate set of  $\lambda$ s for false positive rates.

Table 1. Group-wise probabilistic equal opportunity losses (means across ten trials). See Appendix C.1 for experimental details and how to interpret these numbers.

	Asian	Black	Hispanic	White
Lexicographic	7.25	7.56	7.92	6.25
Max-min	7.25	9.09	8.08	7.80
Full repair (SDP)	28.55	39.14	23.54	23.67
Unrepaired	29.87	42.09	29.72	34.49

Table 1 shows the probabilistic equal opportunity loss on the unrepaired scores, the fully-repaired scores, and the scores computed with the lexicographic and maxmin solutions. In this case, the model developer seeks to ensure equal true positive rates across groups for all thresholds. The lexicographic solution achieves the smallest loss for every group compared to other repair methods. The max-min solution is the second most effective, but is dominated by the lexicographic solution. The full-repair solution, which achieves distributional parity with respect to positive rates, highlights the issues with strong demographic parity as a fair desideratum—the SDP solution has groupwise losses on the order of the unrepaired scores, indicating that a demographic parity based intervention may not be the most effective. The unrepaired scores are several orders of magnitude worse than the repaired scores.

## 6 DISCUSSION & FUTURE RESEARCH

In this paper, we introduce a flexible post-processing method for minimizing distributional disparities across various definitions of fairness, and over all possible downstream choices of a classification threshold. On a technical level (1) we demonstrate how to achieve measures of distributional fairness other than (strong) demographic parity; (2) we show how to achieve fairness over thresholds for the case when the sensitive attribute takes on more than two attributes.

Here, we highlight a few potentially fruitful directions of future work. One limitation of this work is that a single repair parameter controls *entire* group-conditional score distributions. In future work, we look to utilize partial optimal transport as a framework for repairing distributions, we may seek to transport only a subset of the overall data. Additionally, we hope to better understand how to locate global minimal repair, and quantify the gap between *local* minima in distributional parity on the geodesic and the *global* minima in Wasserstein space. Finally, given that the

distributions of both model predictions and ground truth may change over time, further exploration of how sensitive our approach is to distribution shifts may be worthwhile—especially since our method relies on model output, rather than model input.

Broadly, we believe this work is a practical contribution to the set of tools available to a fair machine learning practitioner. Ongoing commentary has criticized the frequent conflation of making predictions and making decisions, especially in the context of fairness [20, 30]; this work is one step towards separating the two.



## REFERENCES

- [1] [n.d.]. Why Inter-Rater Reliability Matters for Recidivism Risk Assessment. <https://bja.ojp.gov/sites/g/files/xyckuh186/files/media/document/pb-interrater-reliability.pdf>
- [2] Rediet Abebe, Solon Barocas, Jon Kleinberg, Karen Levy, Manish Raghavan, and David G. Robinson. 2020. Roles for Computing in Social Change. In *Proceedings of the 2020 Conference on Fairness, Accountability, and Transparency* (Barcelona, Spain) (FAT\* '20). Association for Computing Machinery, New York, NY, USA, 252–260. <https://doi.org/10.1145/3351095.3372871>
- [3] Alekh Agarwal, Alina Beygelzimer, Miroslav Dudík, John Langford, and Hanna Wallach. 2018. A reductions approach to fair classification. In *International Conference on Machine Learning*. PMLR, 60–69.
- [4] Martial Agueh and Guillaume Carlier. 2011. Barycenters in the Wasserstein space. *SIAM Journal on Mathematical Analysis* 43, 2 (2011), 904–924.
- [5] Solon Barocas, Moritz Hardt, and Arvind Narayanan. 2019. *Fairness and Machine Learning*. fairmlbook.org. <http://www.fairmlbook.org>.
- [6] Rachel KE Bellamy, Kuntal Dey, Michael Hind, Samuel C Hoffman, Stephanie Houde, Kalapriya Kannan, Pranay Lohia, Jacquelyn Martino, Sameep Mehta, Aleksandra Mojsilovic, et al. 2018. AI Fairness 360: An extensible toolkit for detecting, understanding, and mitigating unwanted algorithmic bias. *arXiv preprint arXiv:1810.01943* (2018).
- [7] Richard Berk, Hoda Heidari, Shahin Jabbari, Matthew Joseph, Michael Kearns, Jamie Morgenstern, Seth Neel, and Aaron Roth. 2017. A convex framework for fair regression. *arXiv preprint arXiv:1706.02409* (2017).
- [8] Sarah Bird, Miro Dudík, Richard Edgar, Brandon Horn, Roman Lutz, Vanessa Milan, Mehrnoosh Sameki, Hanna Wallach, and Kathleen Walker. 2020. Fairlearn: A toolkit for assessing and improving fairness in AI. *Microsoft, Tech. Rep. MSR-TR-2020-32* (2020).
- [9] Amanda Bower, Sarah N. Kitchen, Laura Niss, Martin J. Strauss, Alexander Vargas, and Suresh Venkatasubramanian. 2017. Fair Pipelines. *arXiv:1707.00391* [cs.CY]
- [10] Felix Brandt, Vincent Conitzer, Ulle Endriss, Jérôme Lang, and Ariel D Procaccia. 2016. *Handbook of computational social choice*. Cambridge University Press.
- [11] Joy Buolamwini and Timnit Gebru. 2018. Gender Shades: Intersectional Accuracy Disparities in Commercial Gender Classification. In *Proceedings of the 1st Conference on Fairness, Accountability and Transparency (Proceedings of Machine Learning Research, Vol. 81)*, Sorelle A. Friedler and Christo Wilson (Eds.). PMLR, 77–91. <https://proceedings.mlr.press/v81/buolamwini18a.html>
- [12] Flavio P Calmon, Dennis Wei, Bhanukiran Vinzamuri, Karthikeyan Natesan Ramamurthy, and Kush R Varshney. 2017. Optimized pre-processing for discrimination prevention. In *Proceedings of the 31st International Conference on Neural Information Processing Systems*. 3995–4004.
- [13] Silvia Chiappa, Ray Jiang, Tom Stepleton, Aldo Pacchiano, Heinrich Jiang, and John Aslanides. 2020. A General Approach to Fairness with Optimal Transport. In *AAAI*. 3633–3640.
- [14] Lenaïc Chizat, Pierre Roussillon, Flavien Léger, François-Xavier Vialard, and Gabriel Peyré. 2020. Faster Wasserstein Distance Estimation with the Sinkhorn Divergence. *arXiv:2006.08172* [math.OC]
- [15] Alexandra Chouldechova. 2016. Fair prediction with disparate impact: A study of bias in recidivism prediction instruments. *arXiv:1610.07524* [stat.AP]
- [16] Evgenii Chzhen, Christophe Denis, Mohamed Hebiri, Luca Oneto, and Massimiliano Pontil. 2020. Fair regression via plug-in estimator and recalibration with statistical guarantees. (2020).
- [17] Evgenii Chzhen, Christophe Denis, Mohamed Hebiri, Luca Oneto, and Massimiliano Pontil. 2020. Fair regression with wasserstein barycenters. *arXiv preprint arXiv:2006.07286* (2020).
- [18] A. Feder Cooper and Ellen Abrams. 2021. Emergent Unfairness in Algorithmic Fairness-Accuracy Trade-Off Research. In *Proceedings of the 2021 AAAI/ACM Conference on AI, Ethics, and Society*. Association for Computing Machinery, New York, NY, USA, 46–54.
- [19] A. Feder Cooper, Benjamin Laufer, Emanuel Moss, and Helen Nissenbaum. 2022. Accountability in an Algorithmic Society: Relationality, Responsibility, and Robustness in Machine Learning. *arXiv:2202.05338* [cs.CY]
- [20] Sam Corbett-Davies and Sharad Goel. 2018. The Measure and Mismeasure of Fairness: A Critical Review of Fair Machine Learning. *CoRR abs/1808.00023* (2018). *arXiv:1808.00023* <http://arxiv.org/abs/1808.00023>
- [21] Emily Diana, Wesley Gill, Ira Globus-Harris, Michael Kearns, Aaron Roth, and Saeed Sharifi-Malvajerdi. 2021. Lexicographically Fair Learning: Algorithms and Generalization. *CoRR abs/2102.08454* (2021). *arXiv:2102.08454* <https://arxiv.org/abs/2102.08454>
- [22] Frances Ding, Moritz Hardt, John Miller, and Ludwig Schmidt. 2021. Retiring Adult: New Datasets for Fair Machine Learning. *arXiv preprint arXiv:2108.04884* (2021).
- [23] Sanghamitra Dutta, Dennis Wei, Hazar Yueksel, Pin-Yu Chen, Sijia Liu, and Kush Varshney. 2020. Is There a Trade-Off Between Fairness and Accuracy? A Perspective Using Mismatched Hypothesis Testing. In *Proceedings of the 37th International Conference on Machine Learning (Proceedings of Machine Learning Research, Vol. 119)*, Hal Daumé III and Aarti Singh (Eds.). PMLR, 2803–2813. <https://proceedings.mlr.press/v119/dutta20a.html>
- [24] Cynthia Dwork, Christina Ilvento, and Meena Jagadeesan. 2020. Individual Fairness in Pipelines. *CoRR abs/2004.05167* (2020). *arXiv:2004.05167* <https://arxiv.org/abs/2004.05167>
- [25] Michael Feldman, Sorelle A Friedler, John Moeller, Carlos Scheidegger, and Suresh Venkatasubramanian. 2015. Certifying and removing disparate impact. In *proceedings of the 21th ACM SIGKDD international conference on knowledge discovery and data mining*. 259–268.
- [26] Jessica Zosa Forde, A Feder Cooper, Kweku Kwegyir-Aggrey, Chris De Sa, and Michael Littman. 2021. Model Selection’s Disparate Impact in Real-World Deep Learning Applications. *arXiv preprint arXiv:2104.00606* (2021).

- [27] Sorelle A Friedler, Carlos Scheidegger, Suresh Venkatasubramanian, Sonam Choudhary, Evan P Hamilton, and Derek Roth. 2019. A comparative study of fairness-enhancing interventions in machine learning. In *Proceedings of the conference on fairness, accountability, and transparency*. 329–338.
- [28] Paula Gordaliza, Eustasio Del Barrio, Gamboa Fabrice, and Jean-Michel Loubes. 2019. Obtaining fairness using optimal transport theory. In *International Conference on Machine Learning*. PMLR, 2357–2365.
- [29] Thibaut Le Gouic, Jean-Michel Loubes, and Philippe Rigollet. 2020. Projection to fairness in statistical learning. *arXiv preprint arXiv:2005.11720* (2020).
- [30] Ben Green and Lily Hu. 2018. The myth in the methodology: Towards a recontextualization of fairness in machine learning. In *Proceedings of the machine learning: the debates workshop*.
- [31] Alex Hanna, Emily Denton, Andrew Smart, and Jamila Smith-Loud. 2020. Towards a Critical Race Methodology in Algorithmic Fairness. In *Proceedings of the 2020 Conference on Fairness, Accountability, and Transparency* (Barcelona, Spain) (FAT\* '20). Association for Computing Machinery, New York, NY, USA, 501–512. <https://doi.org/10.1145/3351095.3372826>
- [32] Moritz Hardt, Eric Price, and Nathan Srebro. 2016. Equality of opportunity in supervised learning. In *Proceedings of the 30th International Conference on Neural Information Processing Systems*. 3323–3331.
- [33] Ursula Hébert-Johnson, Michael Kim, Omer Reingold, and Guy Rothblum. 2018. Multicalibration: Calibration for the (computationally-identifiable) masses. In *International Conference on Machine Learning*. PMLR, 1939–1948.
- [34] Shlomi Hod. 2018–. Responsibly: Toolkit for Auditing and Mitigating Bias and Fairness of Machine Learning Systems. <http://docs.responsibly.ai/>
- [35] Anna Lauren Hoffmann. 2019. Where fairness fails: data, algorithms, and the limits of antidiscrimination discourse. *Information, Communication & Society* 22, 7 (2019), 900–915.
- [36] John N Hooker. 2010. Optimality conditions for distributive justice. *International Transactions in Operational Research* 17, 4 (2010), 485–505.
- [37] Lily Hu and Yiling Chen. 2020. Fair Classification and Social Welfare (FAT\* '20). Association for Computing Machinery, New York, NY, USA, 535–545. <https://doi.org/10.1145/3351095.3372857>
- [38] Ray Jiang, Aldo Pacchiano, Tom Stepleton, Heinrich Jiang, and Silvia Chiappa. 2020. Wasserstein fair classification. In *Uncertainty in Artificial Intelligence*. PMLR, 862–872.
- [39] Faisal Kamiran and Toon Calders. 2012. Data preprocessing techniques for classification without discrimination. *Knowledge and Information Systems* 33, 1 (2012), 1–33.
- [40] Faisal Kamiran, Asim Karim, and Xiangliang Zhang. 2012. Decision theory for discrimination-aware classification. In *2012 IEEE 12th International Conference on Data Mining*. IEEE, 924–929.
- [41] Michael Kearns, Seth Neel, Aaron Roth, and Zhiwei Steven Wu. 2018. Preventing fairness gerrymandering: Auditing and learning for subgroup fairness. In *International Conference on Machine Learning*. PMLR, 2564–2572.
- [42] Michael P Kim, Amirata Ghorbani, and James Zou. 2019. Multiaccuracy: Black-box post-processing for fairness in classification. In *Proceedings of the 2019 AAAI/ACM Conference on AI, Ethics, and Society*. 247–254.
- [43] Jon Kleinberg. 2018. Inherent Trade-Offs in Algorithmic Fairness. (2018), 40. <https://doi.org/10.1145/3219617.3219634>
- [44] Preethi Lahoti, Alex Beutel, Jilin Chen, Kang Lee, Flavien Prost, Nithum Thain, Xuezhi Wang, and Ed H. Chi. 2020. Fairness without Demographics through Adversarially Reweighted Learning. *CoRR* abs/2006.13114 (2020). arXiv:2006.13114 <https://arxiv.org/abs/2006.13114>
- [45] Anton Mallasto and Aasa Feragen. 2017. Learning from uncertain curves: The 2-Wasserstein metric for Gaussian processes. In *Advances in Neural Information Processing Systems*, I. Guyon, U. V. Luxburg, S. Bengio, H. Wallach, R. Fergus, S. Vishwanathan, and R. Garnett (Eds.), Vol. 30. Curran Associates, Inc. <https://proceedings.neurips.cc/paper/2017/file/7a006957be65e608e863301eb98e1808-Paper.pdf>
- [46] Ashlyn Aiko Nelson. 2010. Credit scores, race, and residential sorting. *Journal of Policy Analysis and Management* 29, 1 (2010), 39–68.
- [47] Ziad Obermeyer and Sendhil Mullainathan. 2019. Dissecting Racial Bias in an Algorithm That Guides Health Decisions for 70 Million People. In *Proceedings of the Conference on Fairness, Accountability, and Transparency* (Atlanta, GA, USA) (FAT\* '19). Association for Computing Machinery, New York, NY, USA, 89. <https://doi.org/10.1145/3287560.3287593>
- [48] Geoff Pleiss, Manish Raghavan, Felix Wu, Jon Kleinberg, and Kilian Q Weinberger. 2017. On Fairness and Calibration. *Advances in Neural Information Processing Systems* 30 (2017), 5680–5689.
- [49] Andrew D. Selbst, Danah Boyd, Sorelle A. Friedler, Suresh Venkatasubramanian, and Janet Vertesi. 2019. Fairness and Abstraction in Sociotechnical Systems. In *Proceedings of the Conference on Fairness, Accountability, and Transparency* (Atlanta, GA, USA) (FAT\* '19). Association for Computing Machinery, New York, NY, USA, 59–68. <https://doi.org/10.1145/3287560.3287598>
- [50] Bahar Taskesen, Jose Blanchet, Daniel Kuhn, and Viet Anh Nguyen. 2021. A Statistical Test for Probabilistic Fairness. In *Proceedings of the 2021 ACM Conference on Fairness, Accountability, and Transparency* (Virtual Event, Canada) (FAccT '21). Association for Computing Machinery, New York, NY, USA, 648–665. <https://doi.org/10.1145/3442188.3445927>
- [51] Robin Vogel, Aurélien Bellet, Stephan Clémen, et al. 2021. Learning Fair Scoring Functions: Bipartite Ranking under ROC-based Fairness Constraints. In *International Conference on Artificial Intelligence and Statistics*. PMLR, 784–792.
- [52] Mikhail Yurochkin, Amanda Bower, and Yuekai Sun. 2019. Training individually fair ML models with sensitive subspace robustness. *arXiv preprint arXiv:1907.00020* (2019).
- [53] Muhammad Bilal Zafar, Isabel Valera, Manuel Gomez Rodriguez, and Krishna P. Gummadi. 2017. Fairness Beyond Disparate Treatment & Disparate Impact. *Proceedings of the 26th International Conference on World Wide Web* (Apr 2017). <https://doi.org/10.1145/3038912.3052660>

- [54] Muhammad Bilal Zafar, Isabel Valera, Manuel Gomez Rodriguez, Krishna P. Gummadi, and Adrian Weller. 2017. From Parity to Preference-based Notions of Fairness in Classification. [arXiv:1707.00010](https://arxiv.org/abs/1707.00010) [stat.ML]
- [55] Meike Zehlike, Francesco Bonchi, Carlos Castillo, Sara Hajian, Mohamed Megahed, and Ricardo Baeza-Yates. 2017. Fair: A fair top-k ranking algorithm. In *Proceedings of the 2017 ACM on Conference on Information and Knowledge Management*. 1569–1578.
- [56] Rich Zemel, Yu Wu, Kevin Swersky, Toni Pitassi, and Cynthia Dwork. 2013. Learning fair representations. In *International conference on machine learning*. PMLR, 325–333.

## A NOTATION

### A.1 Glossary of Symbols

Below is a glossary of the notation we use in this paper. Symbols generally appear in this table in the order they appear above.

Symbol	Description
$g \in \mathcal{G}$	Set of protected groups
$x \in \mathcal{X}$	Feature space
$y \in Y$	Label space
$D$	A dataset consisting of features, protected attributes, and labels
$\Omega$	The output space of some regressor $f$
$f$	An (unrepaired) regressor
$X, G, Y$	Bold-faced notation expresses random variables
$\tau$	A classification threshold
$\hat{y}$	Classifications generated from thresholding regressor output
$\Gamma_f$	The set of metrics for a regressor $f$ . See Table 2.
$\gamma$	A metric from the confusion matrix for $f$ s.t. $\gamma \in \Gamma_f$ . See Table 2.
$\gamma_{g,k}^{y,c}$	How we notate metrics: $y$ for label, $c$ for class, $g$ for group, and $k$ for index
$\mathcal{P}_p(\Omega)$	Space of Borel probability measures over $\Omega$ with finite $p^{th}$ moments
$\mu, \nu$	Some probability measures, usually in $\mathcal{P}_p(\Omega)$ . Often $\mu_g$ denotes group-specific score distribution.
$\pi_\mu$	The probability density function (PDF) of a measure $\mu$
$\mathcal{W}_p(\mu, \nu)$	p-Wasserstein Distance between $\mu, \nu$
$T \in \mathcal{T}$	The set of transport plans
$F_\mu$	The Cumulative Distribution Function of $\mu$
$F_\mu^{-1}$	The inverse of the CDF; occasionally this is a psuedo-inverse.
$c(\cdot, \cdot)$	A cost function
$\beta$	The Wasserstein barycenter of some measures
$U(\Omega)$	Uniform Distribution on $\Omega$
$\alpha(x, g)$	Like a CDF inverse, but for a regressor
$f_\beta$	The regressor corresponding to total repair with a barycenter $\beta$
$t(x, g)$	The ‘‘shift’’ function used in geometric repair
$\lambda$	Geometric repair parameter, sometimes used to parametrize a barycenter
$f_\beta^\lambda$	A geometrically repaired regressor
$\eta$	Wasserstein geodesic
$\beta_\lambda$	The set of barycenters between two measures, enumerated by geodesic as parametrized by $\lambda$
$\mu_\lambda$	Geometrically repaired score distribution, usually used in tandem with $f_\beta^\lambda$
$\mathcal{H}$	A hypothesis class
$L_g$	The loss for group $g$
$\mathcal{O}$	A bijection ordered group error rates (error as measured by loss function)
$\epsilon$	The error rate at some round of lexicographic, sometimes indexed by $k$
$\Lambda_\ell$	The space of lexicographically fair repair parameters

### A.2 $\gamma$ -Notation for the Confusion Matrix

We also include a table to help better understand our  $\gamma$  notation on confusion matrix based metrics.

Performance Metric	Definition	$\Gamma_f$ -Notation
Positive Selection Rate (PR)	$\Pr[\hat{Y}(\tau) = 1 G = g]$	$\gamma_g^{c=1}(\tau)$
True Positive Rate (TPR)	$\Pr[\hat{Y}(\tau) = 1 Y = 1, G = g]$	$\gamma_g^{1,1}(\tau)$
False Positive Rate (FPR)	$\Pr[\hat{Y}(\tau) = 1 Y = 0, G = g]$	$\gamma_g^{0,1}(\tau)$
Negative Rate (NR)	$\Pr[\hat{Y}(\tau) = 0 G = g]$	$\gamma_g^{c=0}(\tau)$
True Negative Rate (TNR)	$\Pr[\hat{Y}(\tau) = 0 Y = 0, G = g]$	$\gamma_g^{0,0}(\tau)$
False Negative Rate (FNR)	$\Pr[\hat{Y}(\tau) = 0 Y = 1, G = g]$	$\gamma_g^{1,0}(\tau)$

Table 2. This chart illustrates how to express standard metrics in the the confusion matrix, but with  $\gamma$ 's.

### A.3 A Note On Borel Probability Measures

In general, when referring to borel measures analytically, we will assume they are non-atomic, and therefore they are supported on the entire measurable space over which they are defined. Specifically, we mean for a measure  $\mu \in \mathcal{P}_p(\Omega)$  that  $\text{supp } \mu = \Omega$  if  $\mu$  is non-atomic. In cases where measures are assumed to be empirical, we do not make this assumption. We do however, remind the reader that the set of non-atomic Borel Probability measures is dense in the set of Borel probability measures, and so often, these Boreal probability measures are indeed non-atomic.

---

#### Algorithm 1 Computing a lexicographically fair partial Wasserstein repair

---

**Input:** Group conditional scores  $f(x, g)$  and Barycenter function  $\beta(x, g)$  and  $\vec{a}, \vec{w}$   
 $\epsilon_1 \leftarrow \infty$   
 Compute  $L_g(\vec{\lambda})$  for each group and order the loss terms  $L_{h(1)} < \dots < L_{h(n)}$   $\triangleright \vec{\lambda} = 0$   
**for** all  $1 \leq k \leq n$  **do**  
    $\lambda_k \leftarrow \arg \min_{\lambda \in \mathbb{R}^n} L_{h(k)}(\vec{\lambda})$  subject to constraints  $C(\epsilon_1 \dots \epsilon_{k-1})$   
    $\epsilon_k \leftarrow \max_{R \in \mathcal{G}, |R|=k} \sum_{g \in R} L_g(\vec{\lambda})$   
**end for**  
**Output:** lexicographic solution  $\lambda_n$  and error rate  $\epsilon_n$

---

## B SUPPLEMENTAL MATERIAL: SECTION 3 (BINARY SENSITIVE ATTRIBUTE)

### B.1 Computing an Optimal $\lambda$ for Geometric Repair

First we show the pseudo-code of the routine we use to compute an optimal geometric repair  $\lambda$ . In practice, we cannot compute an expectation over all thresholds, so empirically, we make use of a set of evenly spaced candidate thresholds. In our experiments we used `np.linspace(0, 1, .01)`.

---

#### Algorithm 2 Computing repair parameter

---

**Input:** A dataset  $D = \{(x_i, g_i, y_i)\}_{i=1}^N$  regressor  $f(x, g)$ , fair regressor  $f_\beta(x, g)$ , performance metrics(s)  $\gamma_{k=1} \dots \gamma_{k=k} \in \Gamma_{(\cdot)_\beta}^\lambda$ , weight vector  $\vec{w} \in \mathbb{R}_{\geq 0}^k$ , and candidate thresholds  $\{\tau_i\}_{i=1}^m \subseteq \Omega$ .  
 Let  $f_\beta^\lambda(x, g) = f(x, g) + \lambda t(x, g)$   
 $\lambda^* \leftarrow \arg \min_{\lambda \in [0, 1]} \sum_{j=1}^k w_j \sum_{i=1}^m \gamma_{k=j, g}(\tau_i) - \gamma_{k=j, g'}(\tau_i)$  subject to  $\gamma_{k, g} \in \Gamma_{f_\beta}^\lambda$   
**Output:** repair parameter  $\lambda^*$

---

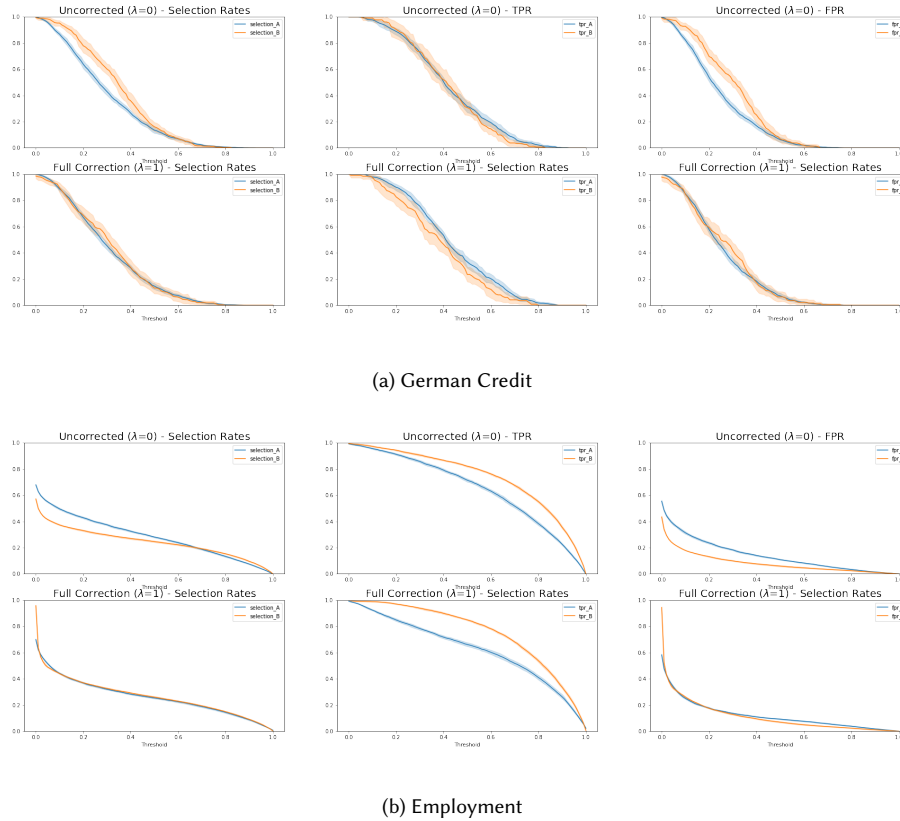


Fig. 7. Group-conditional selection rate, TPR, and FPR curves over thresholds. In each plot, the first row illustrates the uncorrected scores, and the second row illustrates the scores after full correction.

## B.2 Experimental setup

For each dataset, we run ten trials of the experiment; all plots (except Figure 4) show the 95% confidence interval given results from all ten trials. In each trial, we set a new random seed (so that  $\text{seed}=1$  iff  $\text{trial}=1$ ). Each trial proceeds as follows:

- (1) **Score generation.** We training our underlying model, a scikit-learn RandomForestClassifier with default parameters. Using the trained classifier, we predict on a separate set of data to get the *scores*. For every instance in this set, we now have information about its label, group membership, and its score. Since this is a postprocessing method, we will assume that some of this data is labeled (which we can access), and some of this data is unlabeled (which we will use to validate our method).
- (2) **Baseline evaluation.** To get a baseline for distributional (un)fairness, for every  $\tau \in \{0, 0.01, 0.02, \dots, 0.98, 0.99, 1.0\}$ , we calculate binary decisions using  $\tau$  as the decision threshold; then, we compute group-conditional selection rates, TPR, and FPR using these decisions.

	Sens. Attr	Prediction Task	Source
Adult (Old)	Sex	High income	UCI
Income	Race	High income	New Adult
Public Coverage	Race	Medicare	New Adult
Employment	Sex	Employed	New Adult
Taiwan Credit	Education	Good Credit	UCI
German Credit	Age	Good Credit	UCI

Table 3. Summary of datasets used for distributional fairness experiments.

- (3) **Calculating the barycenter adjustment.** Calculating the barycenter adjustment does not require access to labels, so this step can use both the labeled and unlabeled data from Step (1). We calculate the barycenter for the two groups. For this computation, we use a vectorized Python implementation of Chzhen et al. [17]’s code. Now, for every row of data from (1), both labeled and unlabeled, we now additionally have its adjustment: a single (signed) number indicating how it should be transformed in order to lie on the barycenter.
- (4) **Finding the best  $\lambda$ .** Finding  $\lambda$  *does* require access to labels, so we now work only with the *labeled* dataset from (1). Each  $\lambda$  corresponds to a single distributional fairness definition, so these steps are done once for TPR and once for FPR. For each row of this dataset, we have access to its label, group membership, score, and adjustment to the barycenter. In actual usage, we suggest either the probabilistic or exact approaches; the empirical approach is extremely—and unnecessarily—computationally intensive. We use the empirical approach in our experiments simply to illustrate the validity of the probabilistic and exact approaches.
- (a) *Finding  $\lambda$  empirically.* On this new test set, for each value of  $\lambda \in \{0, 0.01, 0.02, \dots, 0.98, 0.99, 1.0\}$ , we multiply  $\lambda$  by the adjustment returned in (3). For each  $\lambda$ , we then follow the evaluation process from (2), and pick the  $\lambda$  that yields the best results (least distributional disparity).
- (b) *Estimating  $\lambda$  probabilistically.* The probabilistic method for finding  $\lambda$  does not require calculating hypothetical decisions. Instead, we apply Proposition 3.10 using the original scores for the numerator and the adjustment found in step 2 for the denominator.
- (c) *Calculating  $\lambda$  exactly.* The exact calculation also does not require calculating hypothetical decisions. We use the standard convex optimization approach implemented from `scipy` (`optimize.minimize_scalar`) to compute the exact  $\lambda$  following the equation in Remark 3.8.
- (5) **Evaluation on unlabeled data.** Our results in Figure 2 illustrate the effect of using the  $\lambda$ s found in (4c) on the *unlabeled* data. Our method makes the assumption that the labeled and unlabeled data are drawn i.i.d. from the same distribution, so it is expected (and unsurprising) that the  $\lambda$ s found using the labeled data are highly effective when applied to the unlabeled data.

### B.3 Datasets

A summary of datasets used for distributional fairness experiments can be found in the table below. For German Credit and Adult (Old), we used the postprocessed versions from Friedler et al. [27], while New Adult datasets are from Ding et al. [22]. All sensitive attributes are binary, with Sex binarized as male-female, Race binarized as white-nonwhite, the Education feature binarized as low education-high education, and Age binarized as young-old.

For all New Adult datasets, data is pulled from the 2018 California 1-Year Person survey. We use the first 30000 examples. Our train-test splits are as follows: 18000 for training the random forest, and the remaining 12000 for our method, of which 6000 are part of the labeled set, and 6000 are part of the unlabeled set.

The UCI Adult dataset has 30162 examples total. We use 15000 examples for training the random forest, 7581 as the unlabeled set, and 6000 for the final unlabeled set.

The UCI Taiwan dataset has 30000 examples, and we make train-test splits identical to the New Adult datasets.

The UCI German dataset has 1000 examples. We use 500 for training the random forest, 250 as the labeled dataset, and 250 as the unlabeled dataset.

## C SUPPLEMENTAL MATERIAL: SECTION 5 (LEXICOGRAPHIC REPAIR)

### C.1 Additional notes on lexicographic fairness.

Lexicographic Fairness has a very strong connection to max-min fairness. Observe that at the first round of minimization, a lexicographically fair solution will identify the group with the largest loss, and then limit the hypothesis class to the set of hypotheses which minimize error on this group, thereby computing a maxmin solution[21].

**DEFINITION C.1.** A hypothesis  $h$  satisfies max-min fairness if  $h \in \mathcal{H}_{mm}$  where  $\mathcal{H}_{mm} = \{h \in \mathcal{H} : L_{O(1)}(h) = \min_{h' \in \mathcal{H}} L_{O(1)}(h')\}$ .

**THEOREM C.2.** Allow  $h_{mm}$  to be some hypothesis which satisfies max-min fairness and  $h_\ell$  to be a lexicographically fair hypothesis with error profiles  $\epsilon(h_{mm})$  and  $\epsilon(h_\ell)$  respectively. Then  $\epsilon(h_{mm}) < \epsilon(h_\ell)$ .

**PROOF.** This theorem follows from the construction of lexicographic solution. By algorithm (1), the loss profile of a lexicographic solution is upper bounded by that of the maxmin solution, as the maxmin solution is produced at round  $j = 1$  and at subsequent rounds, is used as an upper bound for remaining optimization rounds. Therefore, if there is ever a round at which the lexicographic solution is not upper bounded by the maxmin solution, the lexicographic solution must no longer be considered lexicographic as it has violated the constraints from round  $j$ .  $\square$

Below is the pseudo code of the algorithm we use to compute a lexicographically fair repair. Here we directly enumerate the constraints for the lexicographic objective rather than make use of no-regret max-min dynamics like [21]. Due to the number of constraints on our optimization problem, we occasionally experience numerical instability issues in our implementation. We look to improve these in future work.

---

#### Algorithm 3 Computing a lexicographically fair repair

---

**Input:** Group conditional scores  $f(x, g)$  and Barycenter function  $\beta(x, g)$  and  $\vec{a}, \vec{w}$

$\epsilon_1 \leftarrow \infty$

Compute  $L_g(\vec{\lambda})$  for each group and order the loss terms  $L_{h(1)} < \dots < L_{h(n)}$

$\triangleright \vec{\lambda} = 0$

**for** all  $1 \leq k \leq n$  **do**

$\lambda_k \leftarrow \arg \min_{\lambda \in \mathbb{R}^n} L_{h(k)}(\vec{\lambda})$  subject to constraints  $C(\epsilon_1 \dots \epsilon_{k-1})$

$\epsilon_k \leftarrow \max_{R \in 2^G, |R|=k} \sum_{g \in R} L_g(\vec{\lambda})$

**end for**

**Output:** lexicographic solution  $\lambda_n$  and error rate  $\epsilon_n$

---



## C.2 Experimental Setup

- (1) **Data generation.** We use the FICO dataset from the responsibly python package [34], documentation for which can be found at docs.responsibly.ai. The FICO dataset is not given in terms of individual data entries. Rather, the dataset is defined in terms of the joint distribution of features, attributes, and labels. The dataset consists of the proportion of individuals with each race, the probability of having some specific credit score given by race, and the likelihood of a missing payment ( $Y=0$ ) for the given race and credit score. The four races in the dataset are Black, White, Hispanic, and Asian. Credit scores are typically between 300 – 850, however in the dataset they are normalized to the interval  $[0, 1]$ . Using the joint distribution over scores, races, and missed payment status, we can generate our own dataset. For our experiments, we use  $8k$  entries total,  $4k$  as “labeled” data (from which  $\lambda$ ’s are calculated) and  $4k$  as our “unlabeled” data (which is illustrated in 6).
- (2) **Computing the barycenter.** We compute the barycenter using the python optimal transport library POT. To compute the barycenter we use the regularized bregman optimal transport solver with a regularization parameter  $10^{-3}$ . The weights used in the computation are the proportion of each race given in the dataset.
- (3) **Lexicographic Solver.** As reported in Diana et al. [21], exact lexicographic solvers suffer from numerical instability issues. To this extent, there are two stabilizing parameters ( $\alpha, \epsilon$ ) that are proposed to help compute a lexicographic optimizer. In our experiment we borrow their stabilized computation and use  $\alpha = 10^{-4}$  and  $\epsilon = 10^{-6}$  as hyper parameters in this routine. We encourage the reader to visit the lexicographic paper for a complete treatment of this optimizer.
- (4) **Trials.** We generate data and compute the following solutions 10 times: Lexicographic (LEX), Max-Min (MM), Strong Demographic Parity (SDP), and Unconstrained(Unconst). The unconstrained method is simply the original data without repair. We compute the groupwise loss function for the probabilistic true positive rate difference function, where  $L_s(\lambda) = \sum_{g' \in \mathcal{G}, g' \neq g} |\mathbb{E}_{x \sim \mathcal{X}_g} [f(x, g) | Y = 1] - \mathbb{E}_{x \sim \mathcal{X}_{g'}} [f(x, g) | Y = 1]|$ , and the same for the probabilistic false positive rate.

## C.3 Interpreting Results

As stated above, the loss function used in the optimizer is based on probabilistic equality in true/false positive rates:  $\mathbb{E}_{x \sim \mathcal{X}} [f(x, g) | Y = 1, G = g]$  or  $\mathbb{E}_{x \sim \mathcal{X}} [f(x, g) | Y = 0, G = g]$ . Practically, this quantity (for a single group) is simply *the average score of examples labeled  $y = 1$* . Then, the “loss” for a single group  $g$  recorded in Table 1/ Table 4 is the sum of every difference between that group’s average score for examples labeled  $y = 1$  and every other group’s average score for examples labeled  $y = 1$ .

Table 4. Group-wise probabilistic equal opportunity losses (means across ten trials). (Replicated from Section 5.)

	Asian	Black	Hispanic	White
Lexicographic	7.25	7.56	7.92	6.25
Max-min	7.25	9.09	8.08	7.80
Full repair (SDP)	28.55	39.14	23.54	23.67
Unrepaired	29.87	42.09	29.72	34.49

Table 5. Group-wise probabilistic equal opportunity losses (standard errors across ten trials)

	Asian	Black	Hispanic	White
Lexicographic	0.85	1.51	1.22	0.78
Max-min	0.80	1.61	1.19	1.05
Full repair (SDP)	1.79	1.27	0.86	0.77
Unrepaired	1.31	2.15	1.21	1.08

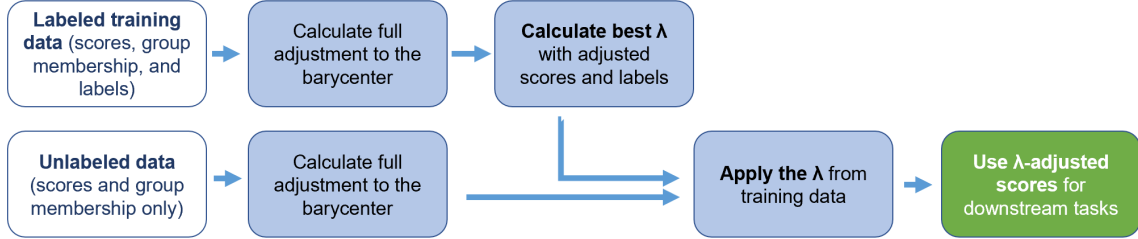


Fig. 8. Figure 5, copied here for convenience.

## D USABILITY

Appendix B.1 roughly follows our anticipated workflow, illustrated in Figure 8.

Our method assumes that a reasonably-well-performing model already exists. We do not need access to the model itself—only its predictions on some labeled data. After calculating how each point’s score would need to change in order to be mapped onto the barycenter, we use that labeled data to calculate the best  $\lambda$  (or  $\vec{\lambda}$ , in case of a non-binary sensitive attribute) for a particular fairness goal (such as equal TPRs, equal FPRs, or see below for more extensions).

Meanwhile, with the unlabeled data on which we want to make adjustments, we use the model to predict scores for this data; then, we make the barycenter calculation to compute the adjustment for each point. Then, we scale those adjustments by the  $\lambda$  or  $\vec{\lambda}$  found from the labeled data. At this point, the scores have been “corrected,” and can be used in downstream applications.

By Corollary 3.7, linear combinations of the  $\gamma \in \Gamma$  that we have defined are also convex in  $\lambda$ . This means that more complex fairness goals can be achieved: for example, equalized odds by considering  $\gamma_g^{1,1}(\tau) + \gamma_g^{0,1}(\tau)$ , or even some less conventional metrics like one which considers both TPR and FPR, but weights TPR more heavily than FPR, or one which considers TPR, FPR, and PR.

### D.1 Suitability

Our experiments hint at a few possible scenarios where our method may be less applicable: (1) when the dataset size is small; (2) when overall disparity is low; and (3) when the relationship between scores and labels is noisier for one group than another. These results suggest that in practice, it is critical to first visualize the threshold curves for both the baseline and full adjustment to determine whether our method is appropriate.

However, in industry production settings, datasets are unlikely to be small; overall low disparity is a good thing, and may mean that no intervention is strictly necessary at all; and finally, if the relationship between scores and labels is noisier for one group than another, this is an indication that the underlying regressor that produced the scores is a

poor hypothesis for the learning task, which means that the model itself should be improved and that papering over its performance with a postprocessing method would be poor practice.

Here, we show results on two datasets, German and Employment, where our method does not perform as well. Figure 7 illustrates group-conditional metrics over all thresholds both before and after the full adjustment to the barycenter is applied, and Figure 9 illustrates the same information as Figure 3.

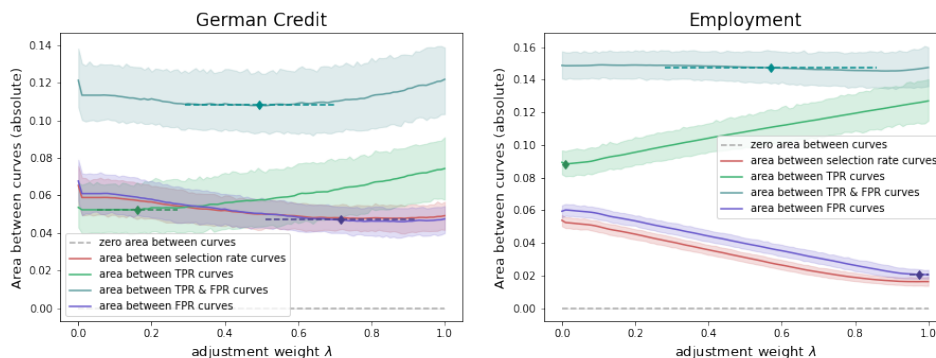


Fig. 9. On the German Credit (left) and Employment (right) datasets: absolute (total) area between the pairs of curves belonging to  $Y_g, Y_{g'}$  after partial repair over possible values of  $\lambda \in [0, 1]$ . Note that these curves do not have the same shape as those in Figure 3: German does not show much variation in disparity across  $\lambda$ , so the minimum is fairly shallow, while the minimums for Employment fall at  $\lambda = 0$  or  $\lambda = 1$ .

**German Credit: small dataset size and low overall disparity.** First, the top row of Figure 7a shows that disparity over thresholds is quite low, even in the uncorrected case. In fact, the TPR curves are approximately overlapping. Applying the barycenter adjustment is successful—the bottom left of Figure 7a indicates that the selection rates have in fact overlapped over all thresholds. Further, note that the TPR and FPR curves, even in the full adjustment with  $\lambda = 1$ , are still extremely close. Consequently, the impact of varying  $\lambda$ , shown in Figure 9, is extremely minimal. Furthermore, the small dataset size resulted in high variability across different train-test splits and therefore extremely wide confidence intervals. In a *single* run, results (both across thresholds and across  $\lambda$ s) were extremely noisy.

**Employment: noisy labels.** The Employment dataset, on the other hand, has plenty of samples since it is from the new Adult dataset. However, taking a closer look at the top row of Figure 7b shows that while the selection rate and FPRs of Group A are higher than those of Group B over almost all thresholds, the TPR of Group A is *lower* than that of Group B over almost all thresholds. Contrast this with the behavior of the uncorrected scores in Figure 2, where the rates for Group A were consistently higher than Group B over all thresholds and for all three metrics. In practical terms, if Group A has a lower TPR and a higher FPR than Group B at all thresholds, this implies that the score-label relationship for Group A is much noisier than the score-label relationship for Group B, which means that merely adjusting the score distributions does not necessarily result in a strictly better or “fairer” set of results. In fact, the full correction (as shown in the bottom left of Figure 7b) is successful in that it results in identical selection rates across all thresholds, as expected, yet looking at Figure 9, it is unclear that a “true” minima for the distance between the TPR curves can be found over  $\lambda \in [0, 1]$ .

## E PROOFS AND PROOF TOOLS

Below are all of these proofs and helping proofs for major results in the paper.

### E.1 External Lemmas (Proofs Omitted)

LEMMA E.1. *This is lemma 6 from [38]. Let  $\mu, \nu \in \mathcal{P}_p(\Omega)$  with differentiable and invertible cumulative distribution function  $F_\mu, F_\nu$  then*

$$\int_{\Omega} F_\mu(x) - F_\nu(x) dx = \int_{\Omega} F_\mu^{-1}(y) - F_\nu^{-1}(y) dy.$$

We remind the reader that  $\Omega = [0, 1]$

LEMMA E.2. *This result is from section 6.1 in [4]. Allow  $\mu_1 \dots \mu_k \in \mathcal{P}_p(\Omega)$  and  $\vec{p} \in \mathbb{R}^k$  to be a weight vector with  $\sum_{i=1}^k p_i = 1$ . The barycenter of these distributions can be defined with respect to one of the distribution  $\mu_j$  with  $1 \leq j \leq k$ . Let  $T_j^i := F_{\mu_i}^{-1} \circ F_{\mu_j}$  then*

$$\beta = \left( \sum_{i=1}^k p_i T_j^i \right)_{\# \mu_j}.$$

From this lemma we learn that (1) mapping onto the barycenter is the result of a linear combination of transportation maps and (2) mass is transported through the use of these transport and the push-forward measure. In other-words, we encourage the reader to view the computation of a new the transported score, and assignment of measure to this score under the barycenter, as the result of separate operations: the transportation map, and the push-forward operator, respectively.

LEMMA E.3. *Fix some distribution  $\nu \in \mathcal{P}_p(\Omega)$ , then the map  $\mu \mapsto \mathcal{W}_p^p(\mu, \nu)$  is convex. This lemma is from [45] Proposition 5.*

### E.2 Proofs of Mathematical Results

**Proposition 2.6.** Let  $f : X \times \mathcal{G} \rightarrow \Omega$  and assume without loss of generality that  $c = 1$ . Then, let  $\mu_{g=0}^y, \mu_{g=1}^y$  be the groupwise distributions of scores  $f$  produces. We have

$$\mathbb{E}_{\tau \in U(\Omega)} |Y_{g=1}^y(\tau) - Y_{g=0}^y(\tau)|^p = \mathcal{W}_p^p(\mu_{g=0}^y, \mu_{g=1}^y). \quad (20)$$

The proof of this result makes use of the following lemma

PROOF. Recall by definition that

$$\begin{aligned} \gamma_g^y(\tau) &= \Pr[\hat{Y}(\tau) = 1 | Y = y, G = g] \\ &= \Pr[f(X, g) \geq \tau | Y = y, G = g] \\ &= 1 - \Pr[f(X, g) \leq \tau | Y = y, G = g] \\ &= 1 - \mu_g^y((-\infty, \tau]) \\ &= 1 - F_{\mu_g^y}(\tau) \end{aligned}$$

Substituting this into the original expectation yields

$$\begin{aligned}
\mathbb{E}_{\tau \in U(\Omega)} |\gamma_{g=1}^y(\tau) - \gamma_{g=0}^y(\tau)|^p &= \int_{\Omega} |\gamma_{g=1}^y(\tau) - \gamma_{g=0}^y(\tau)|^p d\tau \\
&= \int_{\Omega} |(1 - F_{\mu_{g=0}^y}(\tau)) - (1 - F_{\mu_{g=1}^y}(\tau))|^p d\tau \\
&= \int_{\Omega} |F_{\mu_{g=1}^y}(\tau) - F_{\mu_{g=0}^y}(\tau)|^p d\tau \\
&= \int_{\Omega} |F_{\mu_{g=1}^y}^{-1}(\tau) - F_{\mu_{g=0}^y}^{-1}(\tau)|^p d\tau = \mathcal{W}_p^p(\mu_{g=0}^y, \mu_{g=1}^y)
\end{aligned}$$

where the second to last equality follows from lemma E.1.  $\square$

**Proposition 2.9.** Let  $f : X \times \mathcal{G} \rightarrow \Omega$  be a regressor define  $\alpha(x, g) = \inf\{a \in \Omega : F_{\mu_{g'}}(a) \geq F_{\mu_g}(f(x, g))\}$  for  $g, g' \in \mathcal{G}$ . With respect to some fair metric  $\gamma_{g=1}^y(\tau)$  their fair regressor  $f_{\beta} : X \times \mathcal{G} \rightarrow \Omega$  is

$$f_{\beta}(x, g) = p_g f(x, g) + (1 - p_g) \alpha(x, g), \quad x \in X_y \quad (21)$$

where  $p_g$  is the likelihood of belong to group  $g$  and  $X_y$  is the set of all elements with labeling  $y$ .

PROOF. Suppose  $\beta$  is the barycenter of  $\mu_{g=0}, \mu_{g=1}$  with weights  $p_g, (1 - p_g)$ . Then, by Proposition 2.6, mapping onto the barycenter achieves distributional parity for  $\gamma_{g=1}^y(\cdot)$ . Now we will show how to compute the mapping from arbitrary  $\mu_g$  to  $\beta$  and show how this is equivalent to computing  $f_{\beta}(\cdot)$ . First, we will recall two facts we make use of in this proof:

- (1) For non-atomic borel measures (see Appendix A.3), where  $\text{supp } \mu_g = \Omega$ , then the pseudo-inverse is well defined, and is a true inverse. This allows us to write  $F_{\mu_g}^{-1}(F_{\mu_g}(f(x, g))) = f(x, g)$ .
- (2) The function  $\alpha(x, g)$  defines a transportation plan, but in the notation of a regressor as  $\alpha(x, g) = F_{\mu_{g'}}^{-1}(F_{\mu_g}(f(x, g)))$  by the definition of  $\alpha(\cdot, \cdot)$  and the pseudo-inverse.

Allow  $q = F_{\mu_g}(f(x, g))$ , then barycentric quantile function is computed

$$\begin{aligned}
F_{\beta}^{-1}(q) &= p_g F_{\mu_g}^{-1}(q) + (1 - p_g) F_{\mu_{g'}}^{-1}(q) \\
&= p_g F_{\mu_g}^{-1}(F_{\mu_g}(f(x, g))) + (1 - p_g) F_{\mu_{g'}}^{-1}(F_{\mu_g}(f(x, g))) \\
&= p_g f(x, g) + (1 - p_g) \alpha(x, g) = f_{\beta}(x, g)
\end{aligned}$$

In the second to last equality, we make use of the above two facts.  $\square$

**Lemma 3.5.** Fix some threshold  $\tau \in \Omega$ . Assume  $F_{\mu_g^{\lambda}}, F_{\mu_{g'}^{\lambda}}$  have continuous first derivatives for all  $\lambda \in [0, 1]$ . If  $F_{\mu_g^{\lambda}}(\tau) \geq F_{\mu_{g'}^{\lambda}}(\tau)$  then  $\gamma_g(\tau)$  decreases monotonically at that threshold with increase in  $\lambda$ , and increases monotonically if  $F_{\mu_g^{\lambda}}(\tau) \leq F_{\mu_{g'}^{\lambda}}(\tau)$ .

PROOF. Allow  $f$  to be a regressor with metrics  $\Gamma_f$ . Fix  $\tau \in [0, 1]$ . We begin by noting that by definition, any  $\gamma_g^{y,c} \in \Gamma_f$  (w.r.t. the threshold  $\tau$ ) is some metric of the form

$$\gamma_g^{y,c}(\tau) = \Pr[\hat{Y}(\tau) = c | Y = y, G = g] = \int_{\mathcal{X}} \mathbb{1}_{f(x,g) \geq \tau} d\mu^*$$

where  $\mu^*$  is  $\mu_g^{y,c}$ . Define  $\mathcal{X}_\tau = \{x \in X : f(x, g) \geq \tau\}$  to be the set of all  $x$  with a score that is above the given threshold. By the definition of the indicator function, we can ignore the measure of all  $x \notin \mathcal{X}_\tau$  function, and re-write

$$\int_{\mathcal{X}} \mathbb{1}_{f(x,g) \geq \tau} d\mu^* = \int_{\mathcal{X}_\tau} d\mu^* = \mu^*(\mathcal{X}_\tau)$$

which is exactly  $Pr_{x \sim \mathcal{X}}(f(x, g) \geq \tau)$  with respect to the measure  $\mu^*$ . If we take the complement of this probability we can obtain

$$Pr_{x \sim \mathcal{X}}(f(x, g) \geq \tau) = 1 - Pr_{x \sim \mathcal{X}}(f(x, g) \leq \tau)$$

Noting that  $Pr_{x \sim \mathcal{X}}(f(x, g) \leq \tau) = \mu^*([-\infty, \tau])$  is the CDF of the regressor scores, we arrive at the equality that  $\gamma(\tau) = 1 - F_{\mu^*}(\tau)$ . This demonstrates the connection between metrics in  $\Gamma_f$  and the confusion matrix.

To determine the monotonicity of  $\gamma(\tau)$  where  $\gamma \in \Gamma_{f\beta}^\lambda$ , we take its partial derivative with respect to  $\lambda$ . First we derive a relationship between scores input to  $\mu_g$  and  $\mu_g^\lambda$ , or equivalently between  $\mu_g$  and  $f_\beta$ . This equivalency follows from the fact that repaired score distributions can be expressed as a barycenter. From Lemma E.2 we have that

$$\beta(x) = \mu_g \left( (1 - \lambda)F_{\mu_g}^{-1}(F_{\mu_g}(x)) + \lambda F_{\mu_{g'}}^{-1}(F_{\mu_g}(x)) \right) = \mu_g \left( (1 - \lambda)x + \lambda F_{\mu_{g'}}^{-1}(F_{\mu_g}(x)) \right) \quad (22)$$

If we allow  $\rho = (1 - \lambda)x + \lambda F_{\mu_{g'}}^{-1}(F_{\mu_g}(x))$  then we can invert this mapping operation and solve for  $x$

$$M(\rho, \lambda) = \frac{\rho - \lambda F_{\mu_{g'}}^{-1}(F_{\mu_g}(x))}{(1 - \lambda)}. \quad (23)$$

with  $x = M(\rho, \lambda)$ . In the above, we view  $\rho$  as where  $x$  lives on the barycenter after a transport mapping is applied, and  $M(\rho, \lambda)$  to be the function which undoes the transportation mapping—in other words, for what value  $x$  does  $\mu_g$  assign same measure as  $\beta$  assigns  $\rho$ ?

Using this inverse mapping, we can take some score distributed according to  $\mu_g^\lambda$  (recalling that barycenters and repaired distributions can be expressed to represent the same distribution) and determine its “source” score under  $\mu_g$  as a function of  $\lambda$ . Let  $\tau = (1 - \lambda)x' + \lambda F_{\mu_{g'}}^{-1}(F_{\mu_g}(x'))$  for  $x' \in [0, 1]$ . Then  $M(\tau, \lambda) = \frac{\tau - \lambda F_{\mu_{g'}}^{-1}(F_{\mu_g}(x'))}{(1 - \lambda)}$  which yields

$$\begin{aligned} \frac{d}{d\lambda} [-F_{\mu_g^\lambda}(\tau)] &= -\frac{\partial}{\partial \lambda} F_{\mu_g}(M(\tau, \lambda)) = \\ -\frac{\partial}{\partial \lambda} \int_{-\infty}^{M(\tau, \lambda)} f_{\mu_g}(t) dt &= -f_{\mu_g}(M(\tau, \lambda)) \frac{\partial}{\partial \lambda} M(\tau, \lambda) = \\ f_{\mu_g}(M(\tau, \lambda)) &\left( \frac{F_{\mu_{g'}}(F_{\mu_g}^{-1}(x')) - x'}{(1 - \lambda)^2} \right) \end{aligned}$$

To determine if this derivative is positive or negative, we look at the two quantities being multiplied on the last line of the above derivation. If we assume that  $\text{supp } \mu_g = [0, 1]$  then  $f_{\mu_g}(\cdot) > 0$  because it is a PDF. Additionally, since the denominator is squared, it is also always positive. This means the sign of the derivative is controlled by the term  $F_{\mu_{g'}}(F_{\mu_g}^{-1}(x')) - x'$  or equivalently  $F_{\mu_{g'}}(F_{\mu_g}^{-1}(x')) - F_{\mu_g}^{-1}(F_{\mu_g}(x'))$ . If  $F_{\mu_{g'}}(F_{\mu_g}^{-1}(x')) - F_{\mu_g}^{-1}(F_{\mu_g}(x')) > 0$  then  $F_{\mu_{g'}}(F_{\mu_g}^{-1}(x')) > x$  and the derivative is positive, indicating that  $\gamma_g^{y,c}$  is increasing. If the inequality switches direction, then  $\gamma_g^{y,c}$  is decreasing. □

**Theorem 3.6** Define  $\delta_{Y_g}(\lambda) := \mathcal{W}_p^p(\mu_g^\lambda, \mu_{g'}^\lambda)$  or equivalently  $\delta_{Y_g}(\lambda) := \mathbb{E}_{\tau \in U(\Omega)} |\gamma_g(\tau) - \gamma_{g'}(\tau)|^p$  for all  $\lambda \in [0, 1]$  and  $\gamma_g \in \Gamma_{f_\beta}^\lambda$ . Then  $\delta_{Y_g}(\lambda)$  is convex.

PROOF. Let  $\lambda_1 \in [0, 1]$  and  $1 - \lambda_1 = \lambda_2$ . By the triangle inequality we have that

$$\mathcal{W}_p^p(\mu_g, \mu_{g'}) \leq \mathcal{W}_p^p(\mu, \mu_g^{\lambda_1}) + \mathcal{W}_p^p(\mu_g^{\lambda_1}, \mu_g^{\lambda_2}) + \mathcal{W}_p^p(\mu_g^{\lambda_2}, \mu_{g'})$$

Since,  $\mu_g^{\lambda_1}, \mu_g^{\lambda_2}$  are all contained on the geodesic between  $\mu_g, \mu_{g'}$  we can obtain equality in the above expression by the following substitution

$$\begin{aligned} \mathcal{W}_p^p(\mu_g, \mu_{g'}) &= \lambda_1 \mathcal{W}_p^p(\mu_g, \mu_{g'}) + (\lambda_2 - \lambda_1) \mathcal{W}_p^p(\mu_g, \mu_{g'}) + (1 - \lambda_2) \mathcal{W}_p^p(\mu_g, \mu_{g'}) \\ &= \mathcal{W}_p^p(\mu, \mu_g^{\lambda_1}) + \mathcal{W}_p^p(\mu_g^{\lambda_1}, \mu_g^{\lambda_2}) + \mathcal{W}_p^p(\mu_g^{\lambda_2}, \mu_{g'}) \end{aligned}$$

since  $\lambda_1 + (\lambda_2 - \lambda_1) + (1 - \lambda_2) = 1$ . Additionally, since  $\mu_g^{\lambda_2}$  lies on the geodesic between  $\mu_g$  and  $\mu_{g'}$ , the following two terms are equivalent  $\mu_{g'}^{\lambda_1} = \mu_g^{\lambda_2}$ . Using this relation and re-arranging terms we arrive at

$$\mathcal{W}_p^p(\mu_g^{\lambda_1}, \mu_{g'}^{\lambda_1}) = \mathcal{W}_p^p(\mu_g, \mu_{g'}) - \mathcal{W}_p^p(\mu_g, \mu_g^{\lambda_1}) - \mathcal{W}_p^p(\mu_{g'}^{\lambda_1}, \mu_{g'})$$

Through observing the following facts, we can conclude the proof. By lemma E.3 we know that  $\mathcal{W}_p^p(\mu_g, \mu_g^{\lambda_1})$  and  $\mathcal{W}_p^p(\mu_{g'}^{\lambda_1}, \mu_{g'})$  are convex. The term  $\mathcal{W}_p^p(\mu_g, \mu_{g'})$  does not depend on  $\lambda$  so we view it as a constant. These facts imply that  $\mathcal{W}_p^p(\mu_g^{\lambda_1}, \mu_{g'}^{\lambda_1})$  is a linear combination of convex functions, which therefore must be also convex. Noting that  $\delta_{Y_g}(\lambda) = \mathcal{W}_p^p(\mu_g^\lambda, \mu_{g'}^\lambda) = \mathbb{E}_{\tau \in U(\Omega)} |\gamma_g(\tau) - \gamma_{g'}(\tau)|^p$  concludes the proof.  $\square$

**Corollary 3.4** A geometrically repaired regressor  $f_\beta^\lambda$  can be computed as the barycenter of  $\mu_g, \mu_{g'}$  with weights  $(1 - \lambda + \lambda p_g)$  and  $\lambda(1 - p_g)$

PROOF. A geometrically repaired regressor is of the form  $f(x, g) + \lambda t(x, g)$ . If we substitute  $t = f_\beta(x, g) - f(x, g)$  into the above expression we obtain

$$\begin{aligned} f(x, g) + \lambda t(x, g) &= \\ f(x, g) + \lambda(f_\beta(x, g) - f(x, g)) &= \\ (1 - \lambda)f(x, g) + \lambda f_\beta(x, g) &= \\ (1 - \lambda)f(x, g) + \lambda(p_g f(x, g) + (1 - p_g)\alpha(x, g)) &= \\ (1 - \lambda + \lambda p_g)f(x, g) + \lambda(1 - p_g)\alpha(x, g) & \end{aligned}$$

Which is identical to the original barycenter computation, but with weight coefficients  $(1 - \lambda + \lambda p_g)$  and  $\lambda(1 - p_g)$ .  $\square$

**Theorem 5.3** For a convex and bounded choice in loss function  $L : \mathbb{R}^n \rightarrow \mathbb{R}$  and convex hypothesis class  $\mathcal{H}$ , Algorithm 3 will output a lexicographically fair solution.

PROOF SKETCH. We proceed by induction. In the base case, we assume that we can compute  $\lambda_1$ , which is minima from the first round of lexicographic optimization i.e. the maxmin solution. This follows by supposition since both the hypothesis class the loss function are bounded and convex. Assume by induction, we can compute the  $k$ th round of optimization

$$\lambda_k \leftarrow \arg \min_{\lambda \in \mathbb{R}^n} L_{h(k)}(\vec{\lambda}) \text{ subject to constraints } C(\epsilon_1 \dots \epsilon_{k-1})$$

optimally subject to the lexicographic constraint set  $C_k(\cdot)$ , and so the resulting  $\lambda_k, \epsilon_k$  satisfies lexicographic fairness. Given that both  $\lambda_k, \epsilon_k$  are lexicographic, then by imposing additional constraints  $C(\epsilon_1 \dots \epsilon_{k-1})$  we are guaranteed that the loss at round  $k + 1$  the solution will be at most as small as the loss at the previous round, thereby satisfying the definition of lexicographic fairness.  $\square$

**Proposition 3.10** The  $\lambda$  which yields the minimum rate difference is given by

$$\lambda = \frac{\mathbb{E}_{\mathcal{X}_{g'}}[f(x, g')|Y, \mathcal{G} = g'] - \mathbb{E}_{\mathcal{X}_g}[f(x, g)|Y, \mathcal{G} = g]}{\mathbb{E}_{\mathcal{X}_g}[t(x, g)|Y, \mathcal{G} = g] - \mathbb{E}_{\mathcal{X}_{g'}}[t(x, g')|Y, \mathcal{G} = g']}$$

PROOF. Suppose there is some value  $\lambda \in [0, 1]$  such that the probabilistic equal opportunity difference between groups is equal

$$\mathbb{E}_{\mathcal{X}_g|Y=1}[f_\beta^\lambda(x, g)] = \mathbb{E}_{\mathcal{X}_{g'}|Y=1}[f_\beta^\lambda(x, g')]$$

We can use the formula for geometric repair to solve for this  $\lambda$ . Recall  $f_\beta^\lambda(x, g) = f(x, g) + \lambda t(x, g)$

$$\begin{aligned} \mathbb{E}_{\mathcal{X}_g|Y}[f(x, g) + \lambda t(x, g)] &= \mathbb{E}_{\mathcal{X}_{g'}|Y}[f(x, g') + \lambda t(x, g')] \\ \mathbb{E}_{\mathcal{X}_g|Y}[f(x, g)] + \lambda \mathbb{E}_{\mathcal{X}_g|Y}[t(x, g)] &= \mathbb{E}_{\mathcal{X}_{g'}|Y}[f(x, g')] + \lambda \mathbb{E}_{\mathcal{X}_{g'}|Y}[t(x, g')] \\ \mathbb{E}_{\mathcal{X}_g|Y}[f(x, g)] + \lambda \mathbb{E}_{\mathcal{X}_g|Y}[t(x, g)] &= \mathbb{E}_{\mathcal{X}_{g'}|Y}[f(x, g')] + \lambda \mathbb{E}_{\mathcal{X}_{g'}|Y}[t(x, g')] \end{aligned}$$

where solving for  $\lambda$  yields the proposition.  $\square$